

## Shear Stress

Even though SED2D did not provide the necessary tools to estimate the long term bed changes in two dimensions due to sediment scour and or deposition, still this modeling exercise was utilized to estimate the spatial distribution of shear stresses for a flow of 45,000 cfs. The spatial shear stresses thus obtained for the ambient conditions and also for all four alternatives are given in Figures 60 through 64, respectively. The shear stress values shown are in SI units and they are given in Kg force per square meter. The conversion factor from Kg force/square meter to pounds per square feet (# force/ft<sup>2</sup>) is 0.205.

An examination of all of these figures will show that the shear stresses at or near the two underwater banks of the navigation channel are relatively higher. Theoretically, this is what is expected for an open channel flow field where with a change in bank slope, a relative increase in shear stress is expected.

## Islands: Bankline Stabilization

The modeling work performed so far can be used to make an estimate of the potential shoreline erosion of the island(s) due to the movement of the water after the islands are built. This type of analysis will only show the potential of erosion due to water movement only. In order to arrive at an estimated area or zones of the island shores where bank stabilization would be needed, the concept of the critical shear or tractive force as it is called or the concept of permissible velocities can be used. There are many textbooks where these values for different particle sizes are given. Table 7 shows some of these values (after Chow 1959). There are other analyses where the critical shear stresses are normally related to the median particle diameter of the bed materials. One such relationship is given by Equation 1 (after Highway Research Board, 1970).

$$\tau_c = 4d_{50} \quad (1)$$

where  $\tau_c$  is the critical shear stress in #/ft<sup>2</sup>, and  $d_{50}$  is in ft.

In engineering design, normally a factor of safety is used to estimate the stable particle size. Factors such as gradation, maximum and minimum sizes, and need of a fitter blanket must also be considered in the design of riprap particles.

The maximum velocities computed for 45,000 cfs next to the islands are in the range of 3 fps. This shows that at some locations, some bank protection work will be needed especially to the side of the island next to the main channel and upstream ends of the island. However, effects of the waves generated by the wind or navigation traffic could finally dictate the need of bank protection work (Bhowmik et. al 1982, Bhowmik 1976, and Bhowmik et. al 1981). Bhowmik et al (1982) computed wind generated wave heights for a sustained wind duration of 6 hours having a frequency of occurrence of 50 years. That analysis for four sites on the Illinois and Mississippi Rivers showed that highest significant wave heights occurred in the month of March and ranged about 0.9 ft for 2-yr wind frequency and 1.6 ft for 50 year wind frequency. Therefore, it is suspected that similar wind waves can be expected also for the Peoria Lake.

Based on this analysis and a knowledge of the expected waves created by commercial and recreational boats, it is almost certain that the right hand side of the islands looking downstream will be subjected to high wave activities either generated by wind or river traffic. In order to protect against such wave activities and also against the zones of high velocities, it is suggested that protective bank stabilization work be installed on all four options at the locations shown in Figures 65, 66, 67, and 68, respectively. These areas or zones of potential protection were agreed on by the USACOE Rock Island District and the Water Survey Scientists based on a telephone discussion. In order to determine the approximate height for which the bank stabilization work along the island shores should be installed, an examination of the long-term water surface changes within the Peoria Lake was performed by the USACOE, Rock Island District (Personal Communication). The USACOE provided the frequency distribution plots of the water surface elevations for the period 1942 through 2000. These frequency plots were developed on a monthly basis and for the 12-month period. The yearly and the Period of Record (POR) frequency plot is shown in Figure 69.

An examination of Figure 69 will show that if the shore lines of the islands as shown in Figures 65 to 68, are stabilized from an elevation of about 439 ft-msl to 443 ft-msl, then the shore lines will be stable against a water surface variation for up to about 82 percent of the time. This means that for about 18 percent of the time, the shorelines will be subjected to water surface activities, which will not have any kind of artificial protective works. It is suggested that the protective works be installed for this zone between elevation variations of 439 ft-msl to 443 ft-msl.

There are numerous techniques that could be used to stabilize the lakeshores, which would be applicable for these islands. These could vary from structural techniques such as rock riprap, gabions, inter-locking blocks, geotubes and others. Non-structural techniques employing Bioengineering should also be suitable for some zones of the island shores. The USACOE will perform the engineering design for the shore stabilization work.

It would be worthwhile to repeat here that in almost all cases, it is expected that the stability of the islands, whether it is at the front ends, or on the west side, will depend on the wave activities whether from wind or river traffic.

### **Velocities Near McClugge Bridge**

Construction of any of these alternatives either upstream or downstream of the McClugge Bridge could alter the flow patterns at or near the bridge. In order to determine the relative changes due to the potential construction of any one of these alternatives, the hydrodynamic modeling results were plotted at a cross section just upstream of the bridge (Figure 70). This illustration shows this cross section, termed Cross Section 7, and the other six cross sections used for island alternatives upstream and downstream of the bridge. The elevations at various locations for this segment of the river are also shown in this figure.

Figures 71 through 74 shows the lateral velocity distributions at this location for all four alternatives for a flow of 45,000 cfs. Each figure shows two velocity distributions, one associated with the ambient condition and one associated with the selected alternative. An examination of these figures will show that except for Alternatives 2, 3, and 4, the changes in velocities are negligible. However, for the Alternatives 2, 3, and 4, the velocity within the navigation channel does increase somewhat with an associated decrease in velocities outside of the navigation channels where most of the bridge piers are located. Therefore, it appears that construction of anyone of these islands should not impact the navigation channel as far as the sedimentation is concerned. At the same time, the altered flow structures due to the island construction would not enhance any scouring at or near the bridge pier.

The model was also ran for a flow of 15,000 cfs. The resulting lateral velocity distributions with and without the island(s) are given in Figures 75 through 78 for Alternatives 1 through 4, respectively. The comparative changes in lateral velocities with and without the islands are similar to those found for a flow of 45,000 cfs, however, with much reduced magnitudes.

This analysis has shown that the velocity structure near the bridge does not change significantly due to the construction of the island except for some increased velocities within the navigation channel and as associated decrease in velocities within the channel border areas.

## **Combined Alternatives**

Based on the environmental and hydrodynamic modeling work, it was decided by the Interagency Committee, that a combination of Alternatives 2 and 3 would provide the maximum habitat benefits. In order to determine the hydrodynamic variabilities when these two alternatives are implemented, hydrodynamic modeling work has been completed for the combined alternatives. The modeling work was completed for 45,000 cfs and 15,000 cfs. The results are given in the following subsections.

### **Alternatives 2 and 3**

These two alternatives were combined assuming that both sets of artificial islands will be built either together or in some type of sequential order. With this set up, the elevations for these two alternatives are depicted in Figure 79. The lateral cross-sections where velocity distributions have been computed are shown in Figure 70. Figure 80 shows the spatial velocity distribution for these two alternatives for a flow of 45,000 cfs. An examination of this figure will show that because of the presence of Alternative 3 in the downstream area, velocities next to Alternative 2 especially on the right (looking downstream) downstream side, do increase somewhat. This slight increase may keep this area relatively clear of sediments. Velocities are quite low at the tips of Alternative 2, right tip of the large island for Alternative 3, and downstream extreme tips of the smaller and larger islands for Alternative 3. It is expected that in the future some sediment accumulation may take place at these locations. Velocities between the two islands for

Alternative 3 are in the range of 0.50 fps to about 1 fps. No low velocities are observed at this area.

The next 7 figures, Figures 81 through 87, show the lateral velocity distributions at cross-sections 1 through 7 (see Figure 70 for cross-section locations) for a flow of 45,000 cfs for combined Alternatives of 2 and 3.

An examination of Figures 81-84 will show that with the combined alternatives, the velocity structures around Alternative 2 changes somewhat to those associated with Alternative 2 only, Figures 19, 20, and 21. The velocities do not increase and or decrease measurably within the main channel. At all three cross-sections there is an increase in velocities next to the island close to the navigation channel. This increase is higher than those observed with Alternative 2 only, Figures 19, 20 and 21.

Figures 84, 85 and 86 show the lateral velocity distributions at cross-sections 4, 5, and 6 (see Figure 70 for cross-section locations). These three cross-sections show the lateral velocity distributions for three cross-sections that pass through Alternative 3. An examination of these three cross-sections will show that the peak velocities within the main channel do increase with the construction of Alternative 2 and 3. This shows that the patterns of sediment deposition within the main channel will not be more than those present for the ambient condition. Except for this slight increase in velocities within the main channel, the lateral velocity structure for this combination and also around Alternative 3 is similar to those observed for Alternative 3 only, Figures 29-31, without the presence of Alternative 2.

The last illustrations for this flow and also for the combined alternatives is Figure 87 which shows the lateral velocity distributions at cross-section 7. Cross-section 7 is located just upstream of the McClugge's Bridge (see Figure 70 for cross-section locations). An examination of this figure and figures 72 and 73 associated individual Alternatives 2 and 3, respectively, will show that the lateral velocity distributions upstream of McClugge's Bridge associated with Alternatives 2 and 3, are similar to those associated with Alternative 3 only. Similar to Figure 73, there is a slight increase in velocities within the main channel and a slight decrease outside of the main channel on the left hand side (east side). This indicates that most of the bridge piers on the east side of the navigation channel will not be subjected to excessive velocities due to the possible construction of these two alternatives.

Figure 88 shows the spatial distributions of shear stresses for a flow of 45,000 cfs for Alternatives 2 and 3. The shear stresses shown are in Kg force per square meter. A comparison of the shear stresses for this combined alternatives to those present with individual alternatives, Figures 62 and 63 for Alternatives 2 and 3, respectively, will show that the patterns of shear stresses are similar even though some enhanced shear stresses are present with the combined alternatives. In all three illustrations, Figures 62, 63, and 88, higher shear stresses associated with the sides of the underwater banks of the navigation channel is quite evident. Theoretically those are the areas where higher shear stresses are expected.

The next seven (7) illustrations, Figures 89-95, show the lateral velocity distributions for a flow of 15,000 cfs at cross-section 1 through 7 (see Figure 70 for cross-section locations), respectively.

Figures 89-91 show the velocities at cross-section 1-3, respectively associated with the zone where Alternative 2 is located. These lateral velocity distributions are similar to those associated with a flow of 45,000 cfs (Figure 81-83). In general, main channel velocity do not change much with the construction of the alternatives and that at cross-section 2, Figure 90, there is a slight increase in velocity next the island near the main channel. Otherwise, the lateral distributions are quite similar to those present with a flow of 45,000 cfs except of course the absolute magnitudes of the velocities for 15,000 cfs are lower than those associated with a flow of 45,000 cfs.

Figures 92-94 show the lateral velocity distributions at cross-sections 4, 5, and 6 respectively (see Figure 70) within the areas where Alternative 3 is located. These lateral distributions of velocities are almost identical to those present for Alternative 3 alone for a flow of 15,000 cfs, see Figures 53, 54 and 55. Of course, the magnitude of the velocities associated with 15,000 cfs are obviously smaller than those associated with a flow of 45,000 cfs.

The last illustration in this series is the lateral velocity distribution at cross-section 7 (see Figure 70) just upstream of the McClugge's Bridge for a flow of 15,000 cfs for these combined alternatives. Again, the distribution of velocities are similar to those present with Alternative 3 alone, Figure 77.

This analysis of the velocities and shear stresses for a flow of 45,000 cfs and 15,000 cfs for the combined Alternatives of 2 and 3 has shown that the:

- Spatial and lateral velocities for the combined alternatives are similar to those present with the individual alternative,
- presence of the islands could slightly increase the velocities within the main channel indicating that sediment deposition and/or scour within the main channel will be similar to those present for the ambient flow conditions.
- velocities upstream of the McClugge's Bridge do not change measurable due to the construction of the islands, thus these islands should not impact the scour and sediment deposition at this location compared to that associated with the ambient flow condition, and
- these two alternatives as well as the individual alternatives could be built without measurably changing the flow patterns within the main channel.

Hydrodynamically, Alternatives 2 and 3 can be built without impacting the river hydraulics measurably. Some areas of the shores of these islands need to be protected as shown in Figures 66 and 67.

## Summary

This letter report has summarized the hydrodynamic modeling work performed by the Illinois State Water Survey in support of the selection of Proposed Artificial Island Construction Sites within the Lower Peoria Lake. Previous studies and new hydrographic data collected by the USACOE have shown that the Peoria Lake has lost a significant amount of its capacity due to sediment deposition. There are several alternatives for the creation of deep-water habitats including the removal of the deposited sediments and placing them at appropriate locations. One of the alternatives is to create artificial islands with the sediments removed from the lakebed. This technique will not only create the needed deep-water habitats outside of the navigation channel, but it will also assist in the placement of dredged materials. Moreover, creation of artificial islands will also recreate terrestrial habitats and zones of lake surface with minimum wave activities which could enhance the reduction of turbidity in those protected areas.

The Illinois State Water Survey in close consultation of the USACOE, Illinois Department of Natural Resources (IDNR) conducted this mathematical hydrodynamic modeling work. The model selected is the two dimensional hydrodynamic unsteady modeling system called RMA 2. This model was calibrated and applied for the entire Peoria Lake with a special emphasis on the Lower Peoria Lake. The Interagency Committee selected the Lower Peoria Lake in and around the McClugge Bridge and on the east side of the navigation channel to be the site where the initial set or sets of islands could be built.

The modeling work was done for two flows, one having a frequency of occurrence of 2-years with a flow of 45,000 cfs. The other was a low flow condition of 15,000 cfs. All model runs were completed for 2-year flow, various alternatives were tested and a final selection of four (4) alternatives were made. Two of these alternatives had islands just upstream of the McClugge Bridge and two below the McClugge Bridge. All proposed islands are located on the east side of the navigation channel.

Modeling work was also completed for a flow of 15,000 cfs with each individual island in place. For all the runs, both for the flows of 45,000 cfs and 15,000 cfs, spatial velocity distributions in two dimensions have been developed and included in this report. A comparative analysis of the lateral velocity distributions at three cross sections, with and without the islands in place, has also been done and the plots included with this report. It was observed that in general, there is some increase in velocities next to the islands along the newly created deep-water channel. The maximum velocities within the main navigation channel do increase in most cases when the island or islands are in place. In one case, some decreases in the velocities were observed when the island was in place.

The height of all the islands was selected to be 450 ft-msl. This will allow top of the islands to be about 3 ft above a 2-year flow. However, for a one percent flow, all the islands will be submerged.

The spatial velocity distributions with the islands in place were reviewed to determine the zones of higher velocities which may require artificial shoreline stabilization work. A review of

the wind generated and river traffic generated waves showed that the bank stabilization work will be needed in some areas essentially against the waves rather than the island induced velocities. Based on a review of the historical water surface variations analyzed by the USACOE, it is suggested that the stabilization work be extended from about 439 ft-msl to 443 ft-msl.

It is suggested that a combination of structural and nonstructural means be considered for stabilizing the selected shore lines against wind and or river traffic generated wave activities and in some cases against the flow induced velocities. The four selected alternatives with deep water channels should enhance aquatic habitats and terrestrial habitats by having a portion of the island(s) above the 2-year stage. Anyone of these islands, if built should also enhance the overall aquatic habitat within the Lower Peoria Lake.

Analyses of the lateral velocity distributions were also performed to determine the changes in velocities that could occur upstream of the McClugge's Bridge due to the construction of anyone of these alternatives. This analysis has shown that if anyone of these islands are built, the velocities within the navigation channel would increase slightly with an associated decrease in velocities within the channel border areas. Thus the bridge piers located within the channel border areas should not be subjected to excess velocities than those expected to be present for the flow conditions without any islands(s).

The last alternative tested is a combined Alternative where alternatives 2 and 3 were jointly modeled. Modeling was done for both flows of 45,000 cfs and 15,000 cfs. Modeling results indicated that construction of these two alternatives, either jointly or sequentially, do not measurably change the spatial or lateral velocity structure around this area of the Lower Peoria Lake compared to those present individually with those alternatives. Thus, Alternatives 2 and 3 can be built without impacting the main channel and the areas just upstream of the McClugge's Bridge.

## **Acknowledgements**

The research results shown here have been completed by the authors and their colleagues at the Illinois State Water Survey as their regular duties. The project is being done as part of the match by the State of Illinois, Department of Natural Resources, to the USACOE. Partial funding for the project was provided by IDNR with John Marlin of the WMRC serving as the Project Coordinator. An extensive amount of support and help was provided by Jim Mick of IDNR. Others who worked as a team and provided a tremendous amount of input are: Brad Thomson, Teresa Kinkaid, Mike Tarpey, Tom Kirkeeng, Mike Schwar of the USACOE. Many Water Survey staff also worked on this project. They are: Pami Parmar, David Soong, Yanging Lian, Bill Bogner, Jim Slowikowski, Susan Shaw, and others. To all of them, the authors express a sincere thank you. The camera-ready copy of this report was prepared by Patti Hill, Becky Howard, and Jenna Dingman.

## References

- Ariathurai, R. 1974. A Finite Element Model for Sediment Transport in Estuaries. Ph.D. Thesis. Department of Civil Engineering, University of California, Davis.
- Ariathurai, R., MacArthur, R.C., and Krone, R.B. 1977 (Oct.). Mathematical Model of Estuarial Sediment Transport. Technical Report D-77-12, U.S. Army Engineer Waterways Experiment Station, Vicksburg, MS.
- Bhowmik, N.G. 1976. Development of Criteria for Shore Protection Against Wind-Generated Waves for Lakes and Ponds in Illinois. University of Illinois Water Resources Center Research Report No. 107. Urbana, IL.
- Bhowmik, N.G., Baur, E., Bogner, W.C., and Demissie, M. 2001. Historical Sedimentation at the Mouths of Five Deltas on Peoria Lake. Illinois State Water Survey Contract Report 2001-08. Champaign, IL.
- Bhowmik, N.G. and M. Demissie. 1989. Sedimentation in the Illinois River and Backwater Lakes. Journal of Hydrology, Vol. 105, No. 1/2, January 30, pp. 187-196.
- Bhowmik, N.G., Demissie, M., and Guo, C-Y. 1982. Waves Generated by River Traffic and Wind on the Illinois and Mississippi Rivers. University of Illinois Water Resources Center Research Report 167, Urbana, IL.
- Bhowmik, N.G., Demissie, M., and Osakada, S. 1981. Waves and Drawdown Generated by River Traffic on the Illinois and Mississippi Rivers. Illinois State Water Survey Contract Report 271, Champaign, IL.
- Bhowmik, N.G., W.C. Bogner, J.A. Slowikowski, and J.R. Adams. 1993. Source Monitoring and Evaluation of Sediment Inputs for Peoria Lake. Illinois Department of Energy and Natural Resources, Research Report ILENR/RE-WR-93/01.
- Chow, V.T. 1959. Open Channel Hydraulics. McGraw-Hill Book Company, Inc. 680 p.
- Demissie, M., Laura Keefer and Renjie Xia. 1992. Erosion and Sedimentation in the Illinois River Basin. Illinois Department of Energy and Natural Resources Report No. ILENR/RE-WR-92/04.
- Demissie, M., and N.G. Bhowmik. 1985. Peoria Lake Sediment Investigation. Illinois State Water Survey Contract Report 371, Champaign, IL.
- Demissie, M., Soong, T.W., and Bhowmik, N.G. 1988. Hydraulic Investigation for the Construction of Artificial Islands in Peoria Lake. Illinois Department of Energy and Natural Resources Report No. ILENR/RE-WR-88/15, Springfield, IL 72P.

National Cooperative Highway Research Program Report. 1970. Tentative Design Procedure for Riprap Lined Channels. Highway Research Board, National Research Council, National Academy of Sciences-National Academy of Engineering.

U.S. Army Corps of Engineers (USACOE). 1992. Illinois River Water Surface Profiles-River Mile 80 to River Mile 290. Rock Island District, Rock Island, Illinois.

**Table 1. Flow Frequencies, Flows and Stages at Chillicothe, After USACOE (1992) RM180**

<i>Flow Frequencies</i>		<i>Flow (cfs)</i>	<i>Stages (ft-msl)</i>
<i>Percent time</i>	<i>Years</i>		
0.2	500	125,000	461.8
0.5	200	114,000	460.2
1.0	100	105,000	459.0
2.0	50	100,000	457.8
4.0	25	85,000	456.4
10.0	10	75,000	454.4
20.0	5	65,000	452.1
50.0	2	45,000	448.4

**Table 2. Flow Frequencies, Flows and Stages at Peoria Lock and Dam; After USACOE (1992)**

<i>Flow Frequency</i>		<i>Flow (cfs)</i>	<i>Stages (ft-msl)</i>
<i>Percent time</i>	<i>Years</i>		
0.2%	500	103,000	460.4
0.5%	200	92,000	459.0
1.0%	100	85,000	457.8
2.0%	50	80,000	456.6
4.0%	25	72,000	455.3
10.0%	10	63,000	453.2
20.0%	5	54,000	451.0
50.0%	2	40,000	447.2

**Table 3. Velocity Changes Due to the Construction of the Island, Alternative 1, Q=45,000 cfs**

<i>Locations</i>	<i>Velocities, fps</i>					
	<i>With Island 1</i>	<i>Without Island 2</i>	<i>With Island 3</i>	<i>Without Island 4</i>	<i>With Island 5</i>	<i>Without Island 6</i>
Cross-section 1	0.08	0.1	0.22	0.21	3.25	3.26
Cross-section 2	0.19	0.19	0.52	0.44	2.77	2.81
Cross-section 3	0.12	0.15	0.32	0.24	2.5	2.51

**Table 4. Velocity Changes Due to the Construction of the Island, Alternative 2,  
Q=45,000 cfs**

<i>Locations</i>	<i>Velocities, fps</i>					
	<i>With Island</i>	<i>Without Island</i>	<i>With Island</i>	<i>Without Island</i>	<i>With Island</i>	<i>Without Island</i>
	<i>1</i>	<i>2</i>	<i>3</i>	<i>4</i>	<i>5</i>	<i>6</i>
Cross-section 1	0.09	0.14	0.42	0.58	2.77	2.8
Cross-section 2	0.08	0.09	0.36	0.32	2.5	2.51
Cross-section 3	0.16	0.09	0.2	0.21	2.45	2.42

**Table 5. Velocity Changes Due to the Construction of the Islands, Alternative 3,  
Q=45,000 cfs**

<i>Locations</i>	<i>Velocities, fps</i>					
	<i>With Island</i>	<i>Without Island</i>	<i>With Island</i>	<i>Without Island</i>	<i>With Island</i>	<i>Without Island</i>
	<i>1</i>	<i>2</i>	<i>3</i>	<i>4</i>	<i>5</i>	<i>6</i>
Cross-section 1	0.77	0.43	0.65	0.55	0.6	0.76
Cross-section 2	0.5	0.47	0.73	0.5	0.77	0.61
Cross-section 3	0.34	0.44	0.75	0.47	0.67	0.54

<i>Locations</i>	<i>With Island</i>	<i>Without Island</i>	<i>With Island</i>	<i>Without Island</i>
	<i>7</i>	<i>8</i>	<i>9</i>	<i>10</i>
	Cross-section 1	1.48	1.47	2.15
Cross-section 2	0.97	1.01	1.79	1.77
Cross-section 3	1	0.81	1.68	1.59

**Table 6. Velocity Changes Due to Construction of An Island, Alternative 4,  
Q=45,000 cfs**

<i>Locations</i>	<i>Velocities, fps</i>					
	<i>With Island</i>	<i>Without Island</i>	<i>With Island</i>	<i>Without Island</i>	<i>With Island</i>	<i>Without Island</i>
	<i>1</i>	<i>2</i>	<i>3</i>	<i>4</i>	<i>5</i>	<i>6</i>
Cross-section 1	0.85	0.45	0.72	0.66	2.05	2.09
Cross-section 2	0.50	0.47	0.68	0.54	1.80	1.77
Cross-section 3	0.32	0.44	0.79	0.49	1.67	1.59

**Table 7. Maximum Permissible Velocities Recommended by Fortier and Scobey  
and the Corresponding Unit-Tractive-Force Values Converted  
by the U.S. Bureau of Reclamation  
(For straight channels of small slope, after aging), See Chow (1959)**

<i>Material</i>	<i>Clear Water</i>		<i>Water transporting colloidal silts</i>	
	<i>V, fps</i>	$\tau_0, \text{lb/ft}^2$	<i>V, fps</i>	$\tau_0, \text{lb/ft}^2$
Fine sand, colloidal	1.50	0.027	2.50	0.075
Sandy loam, noncolloidal	1.75	0.037	2.50	0.075
Silt loam, noncolloidal	2.00	0.048	3.00	0.11
Alluvial silts, noncolloidal	2.00	0.048	3.50	0.15
Ordinary firm loam	2.50	0.075	3.50	0.15
Volcanic ash	2.50	0.075	3.50	0.15
Stiff clay, very colloidal	3.75	0.26	5.00	0.46
Alluvial silts, colloidal	3.75	0.26	5.00	0.46
Shales and hardpans	6.00	0.67	6.00	0.67
Fine gravel	2.50	0.075	5.00	0.32
Graded loam to cobbles when noncolloidal	3.75	0.38	5.00	0.66
Graded silts to cobbles when colloidal	4.00	0.43	5.50	0.80
Coarse gravel, noncolloidal	4.00	0.30	6.00	0.67
Cobbles and shingles	5.00	0.91	5.50	1.10

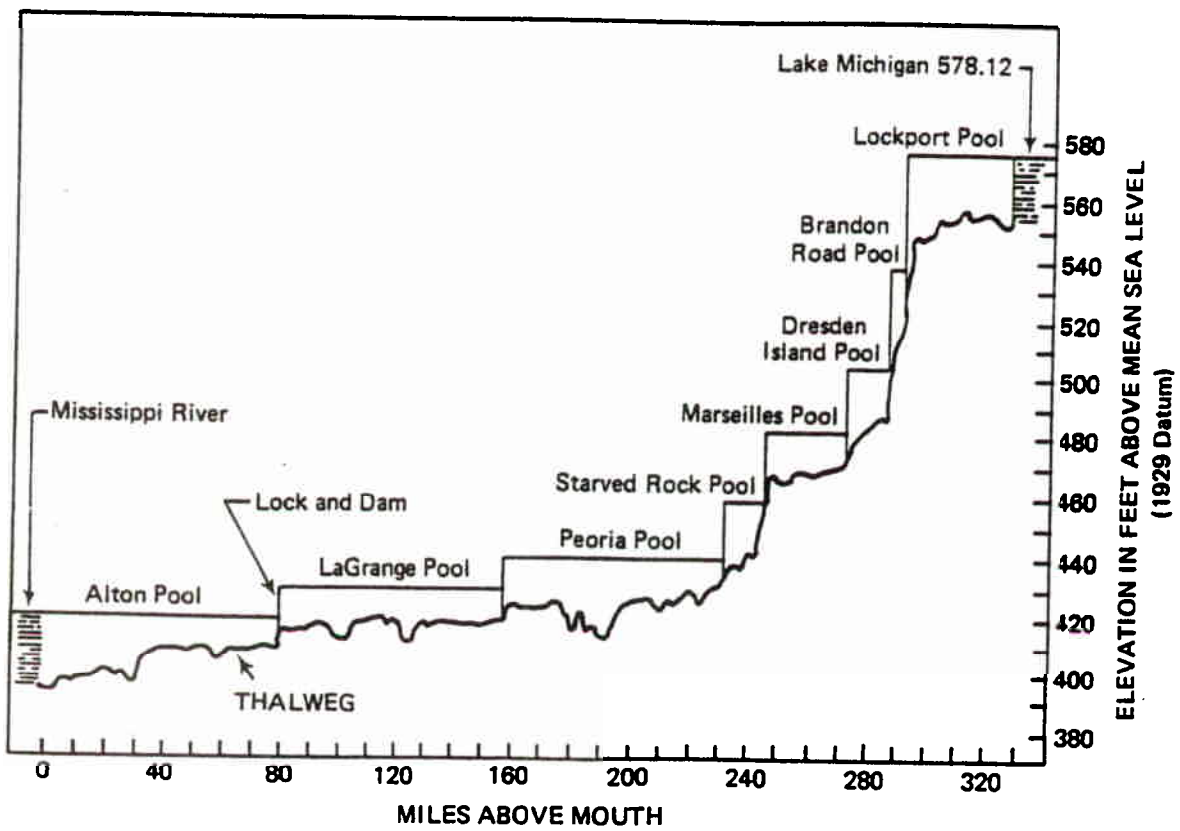


Figure 1. Profile of Illinois River Waterway

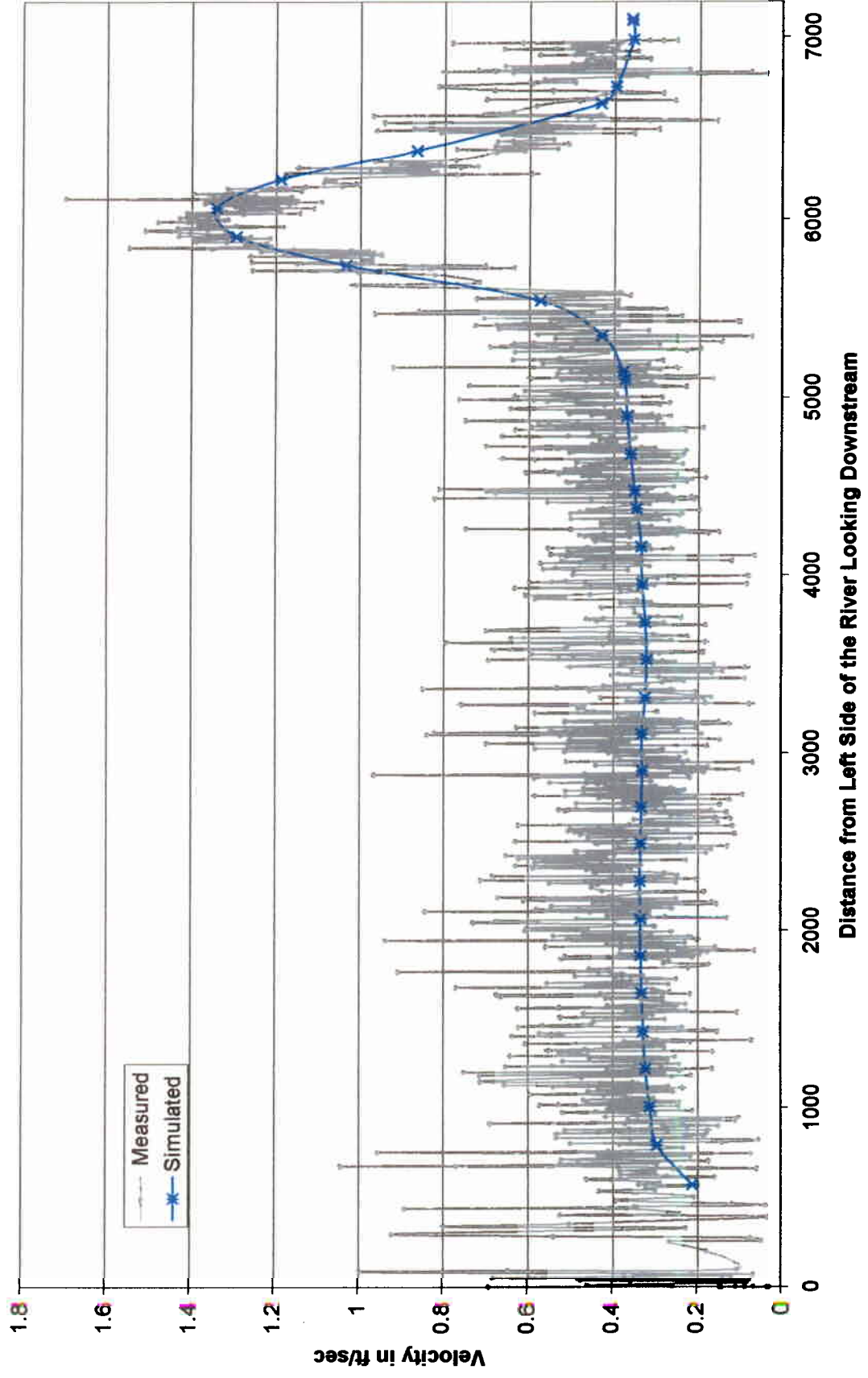


Figure 2. Comparison of the measured and simulated lateral velocity distributions at RM 163.7 (about) for a flow of 25,000 cfs

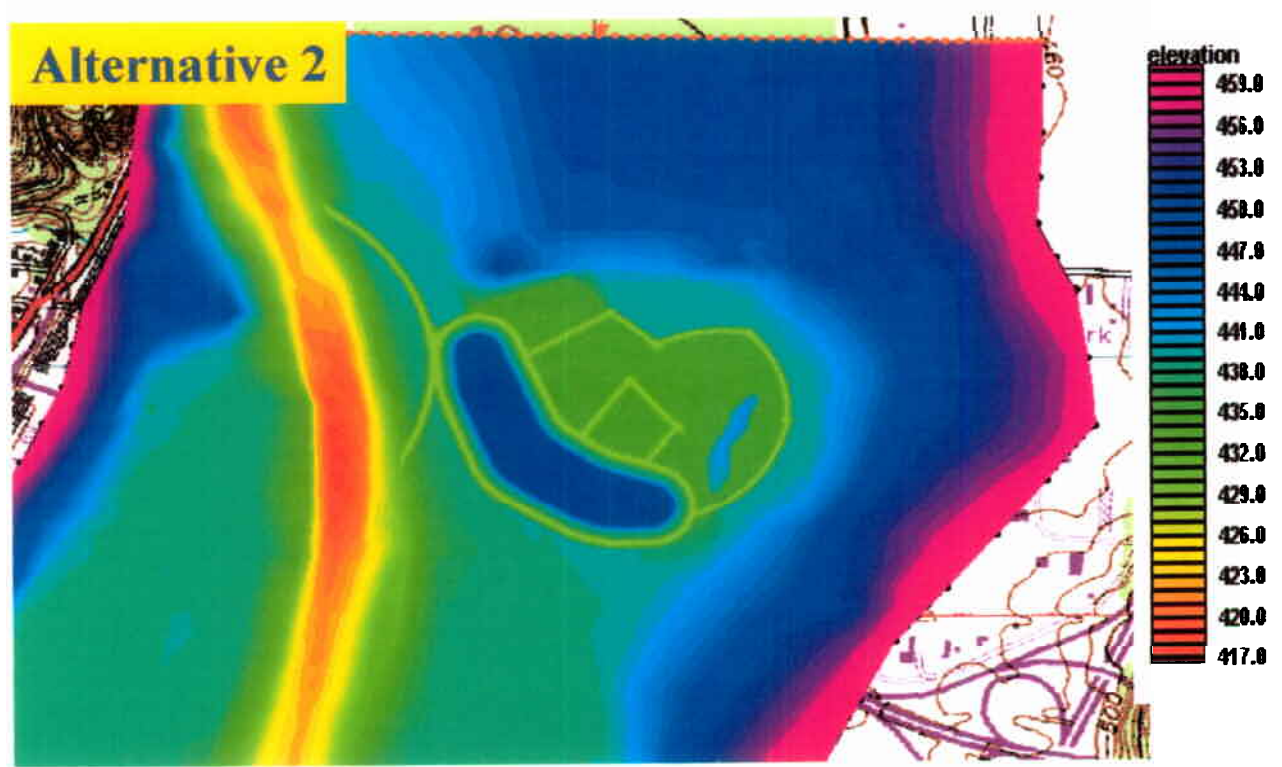
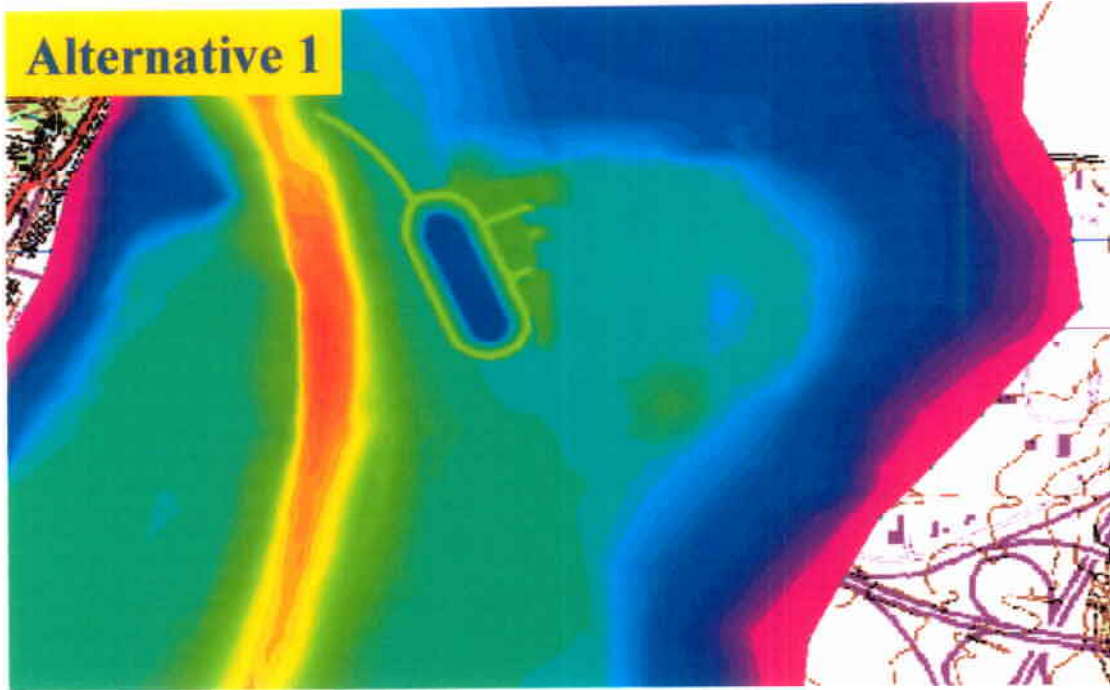


Figure 3. Plan View of Artificial Island Alternatives 1 and 2

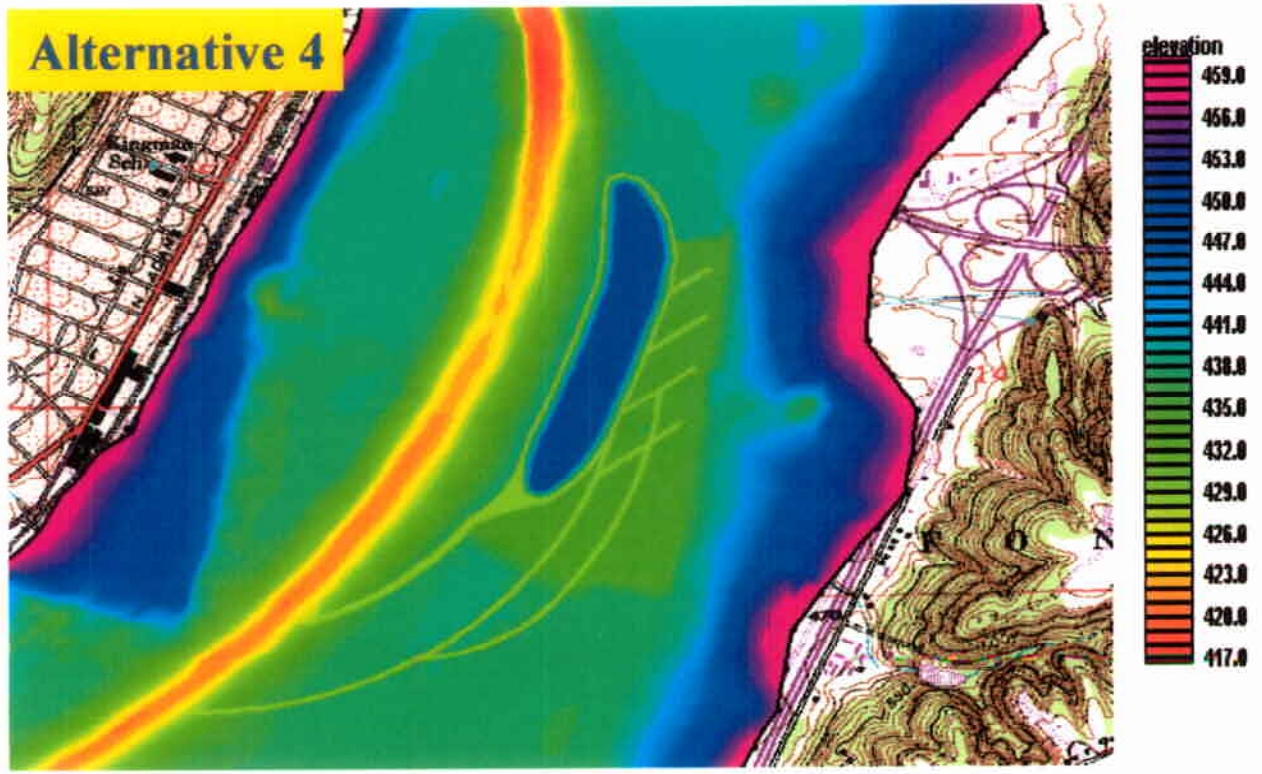
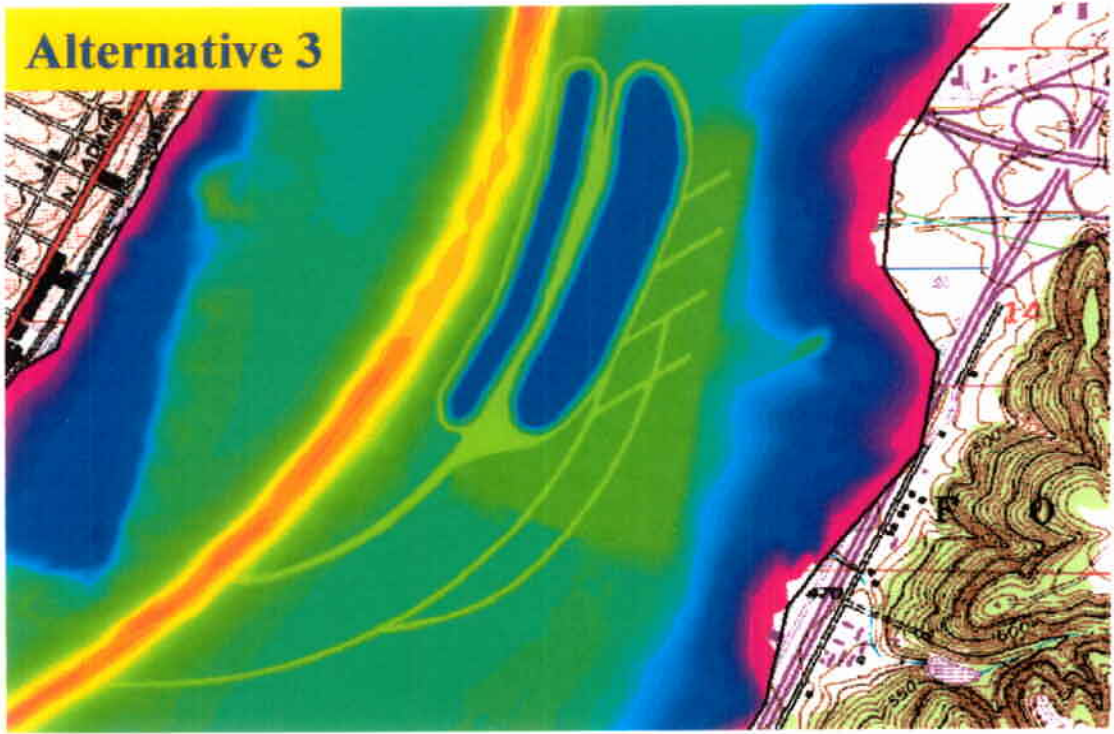


Figure 4. Plan View of Artificial Island Alternatives 3 and 4

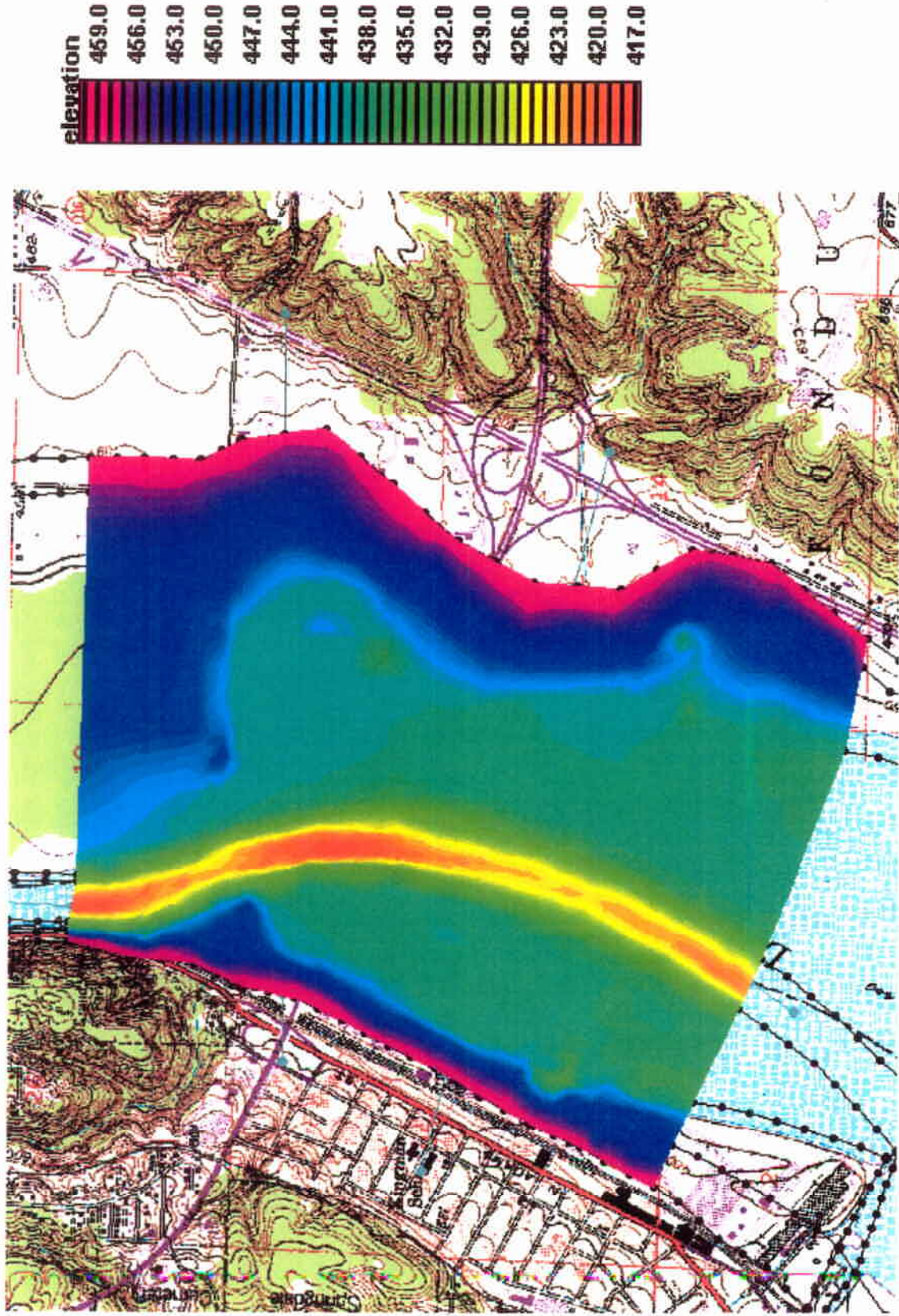


Figure 5. Elevation Variations of the Modeled Area

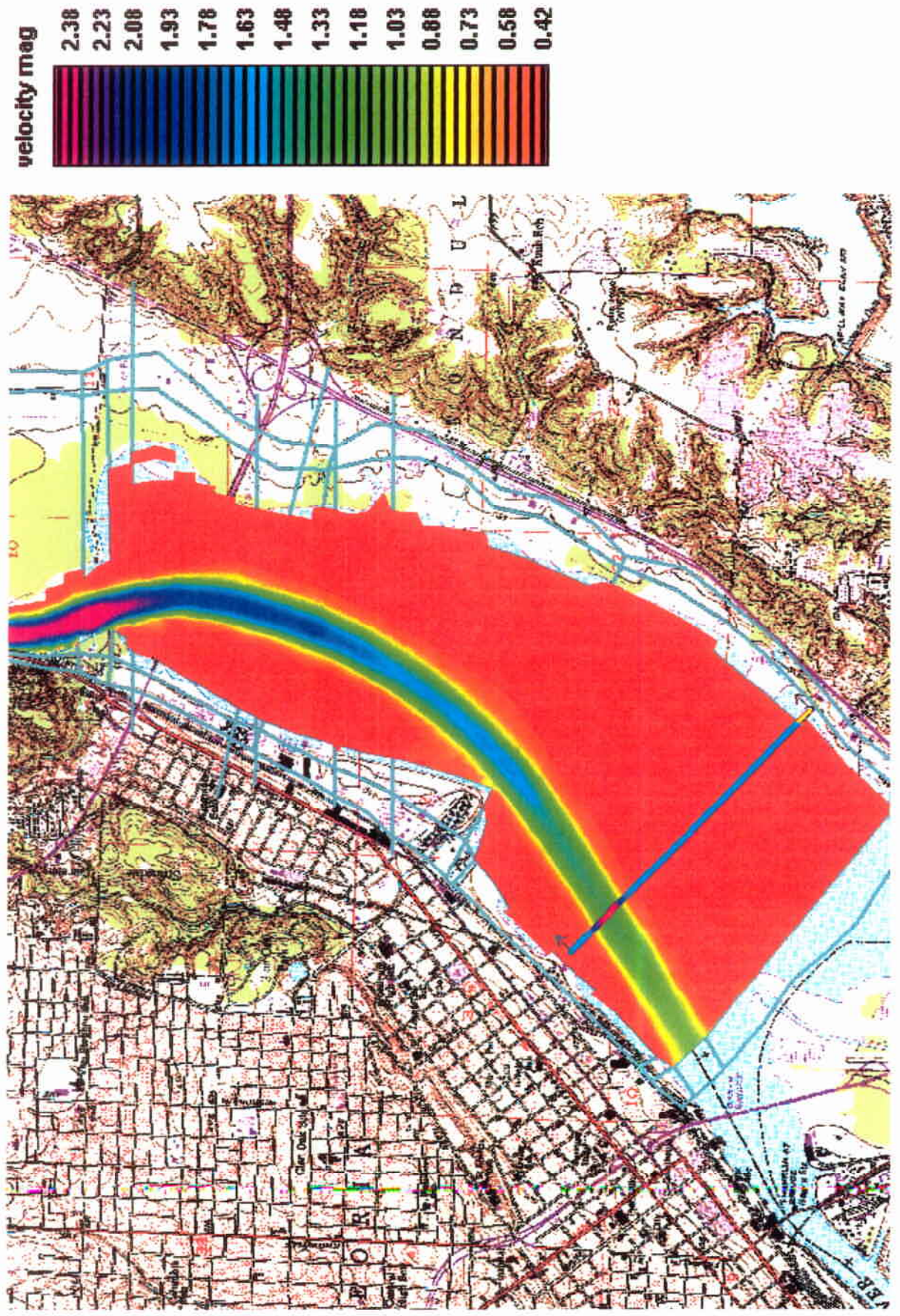


Figure 6. Spatial Velocity Distributions for a flow of 25,000 cfs (Velocity values are in fps)

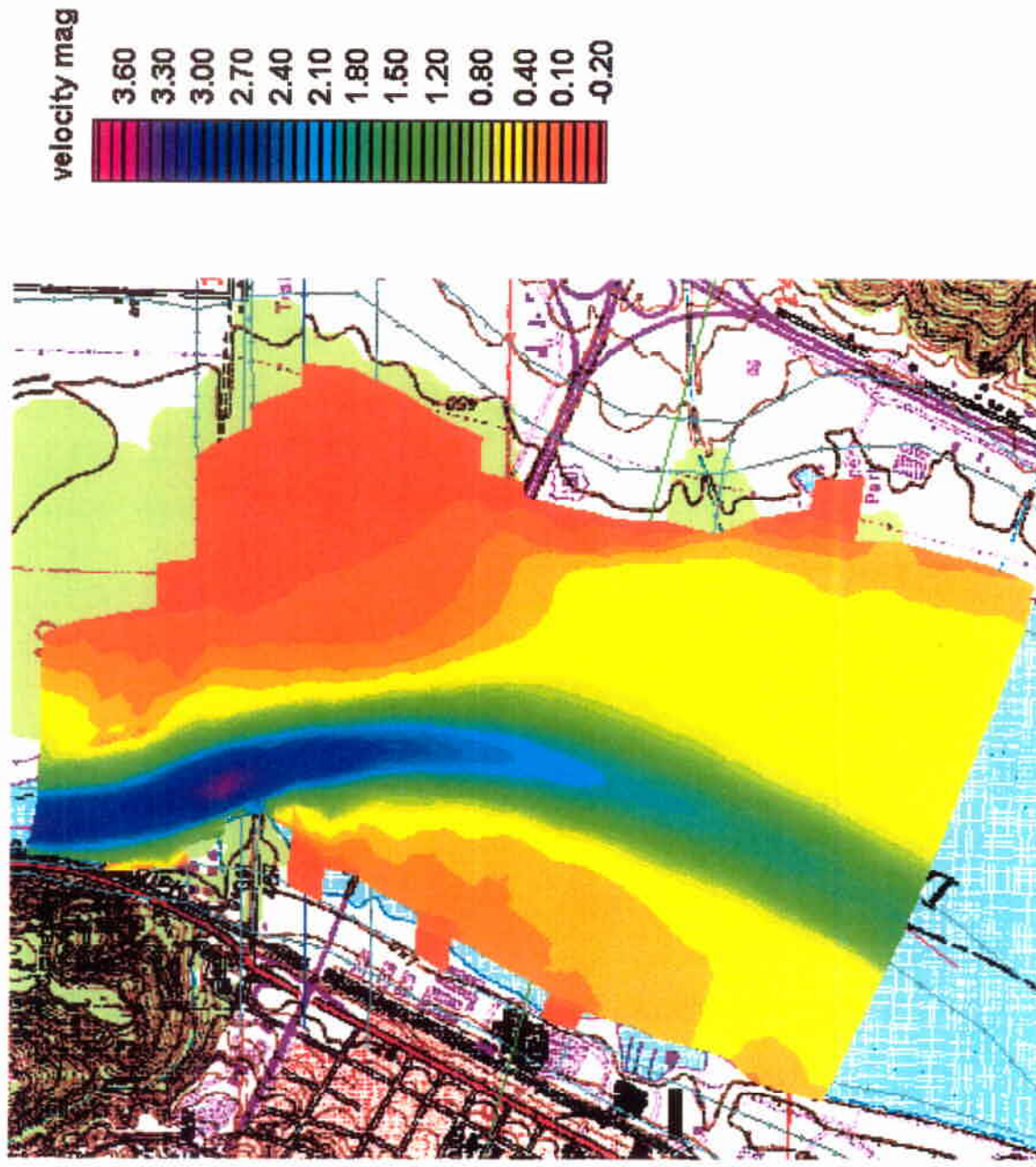


Figure 7. Spatial Velocity Distribution for a flow of 45,000 cfs (Velocities are in fps.)

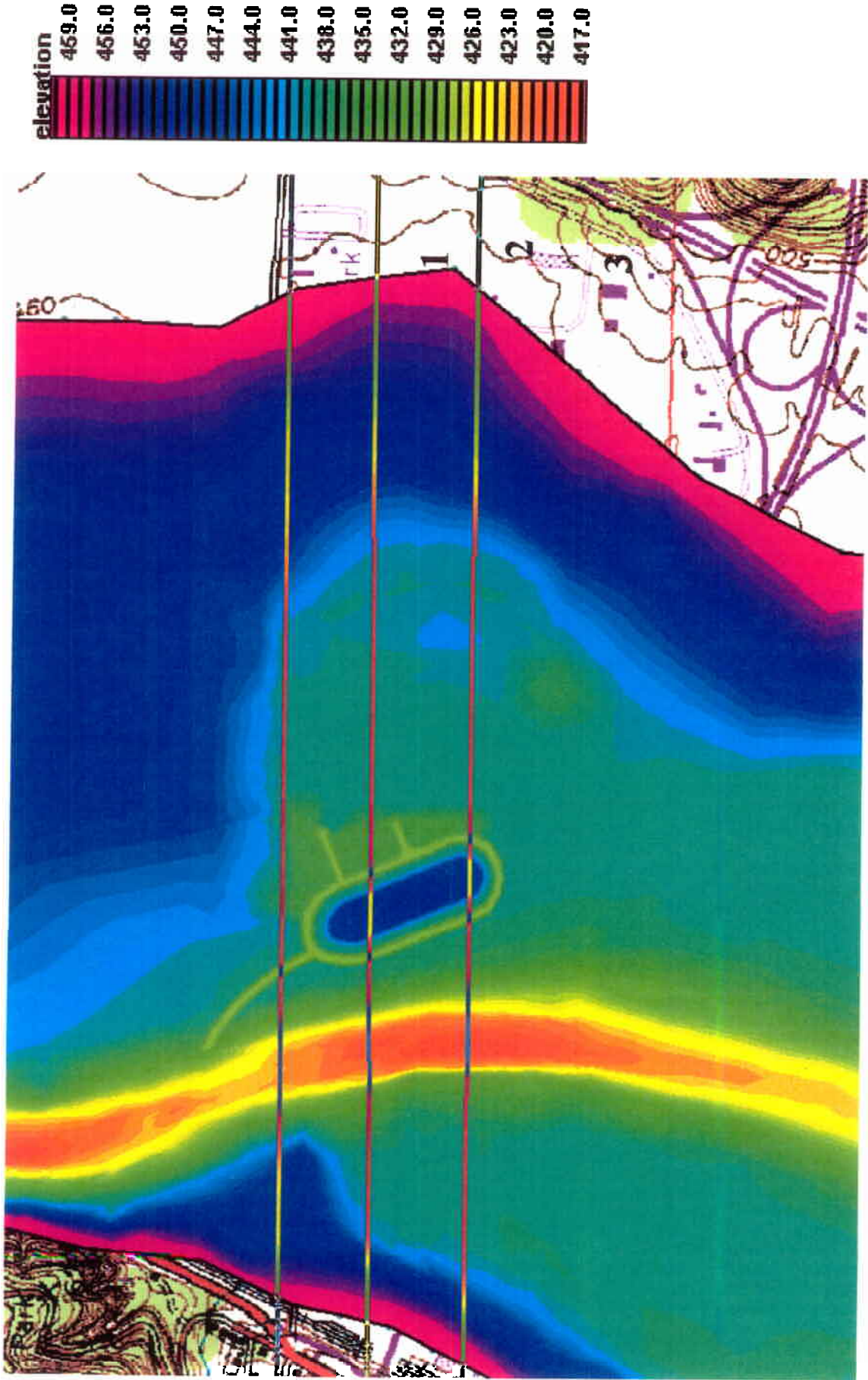


Figure 8. Elevation Map of the Lake with Alternative 1 and Newly Created Deep Water Area

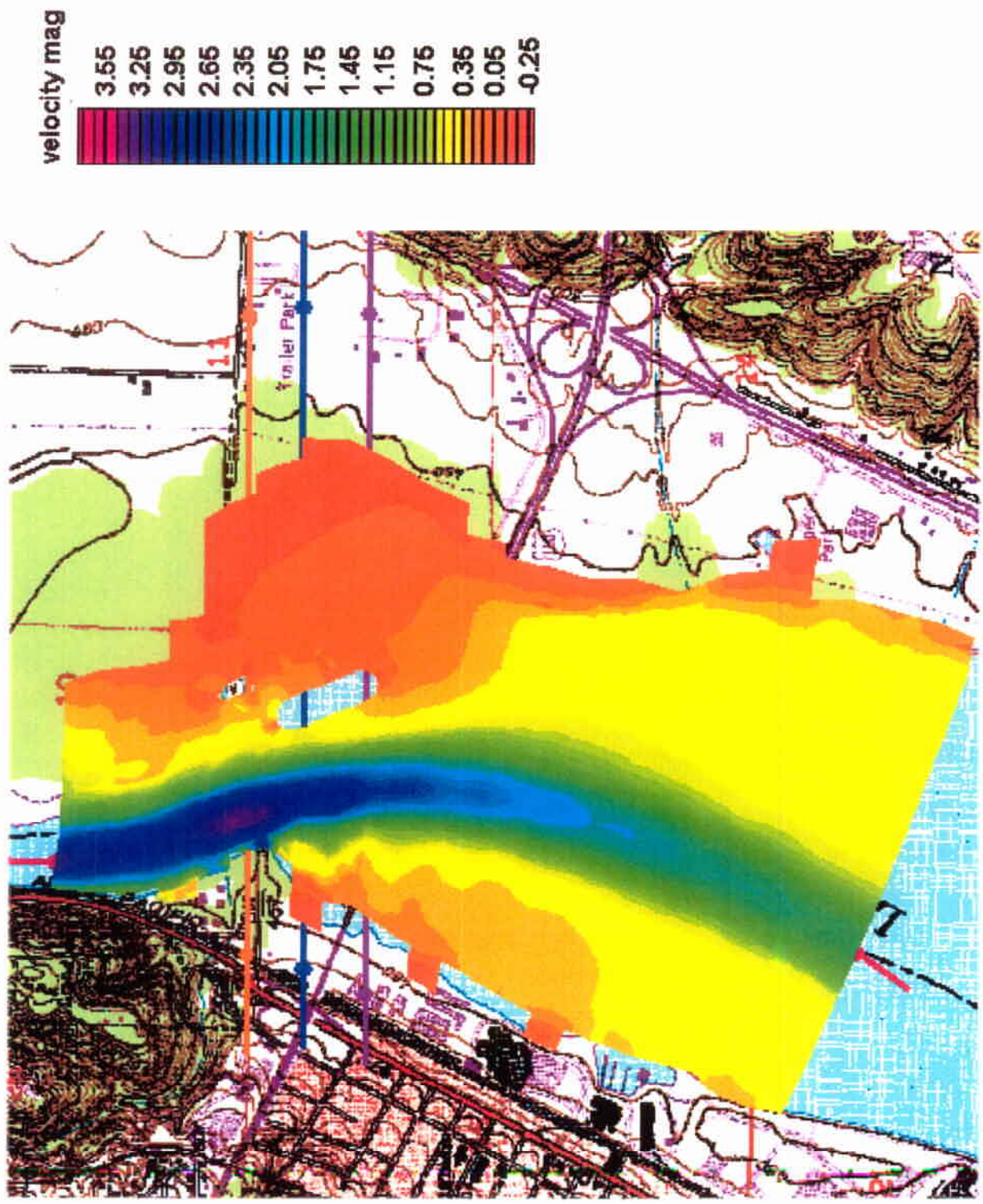


Figure 9. Spatial Velocity Distribution for a flow of 45,000 cfs for Alternative 1  
 (Velocities are in fps)

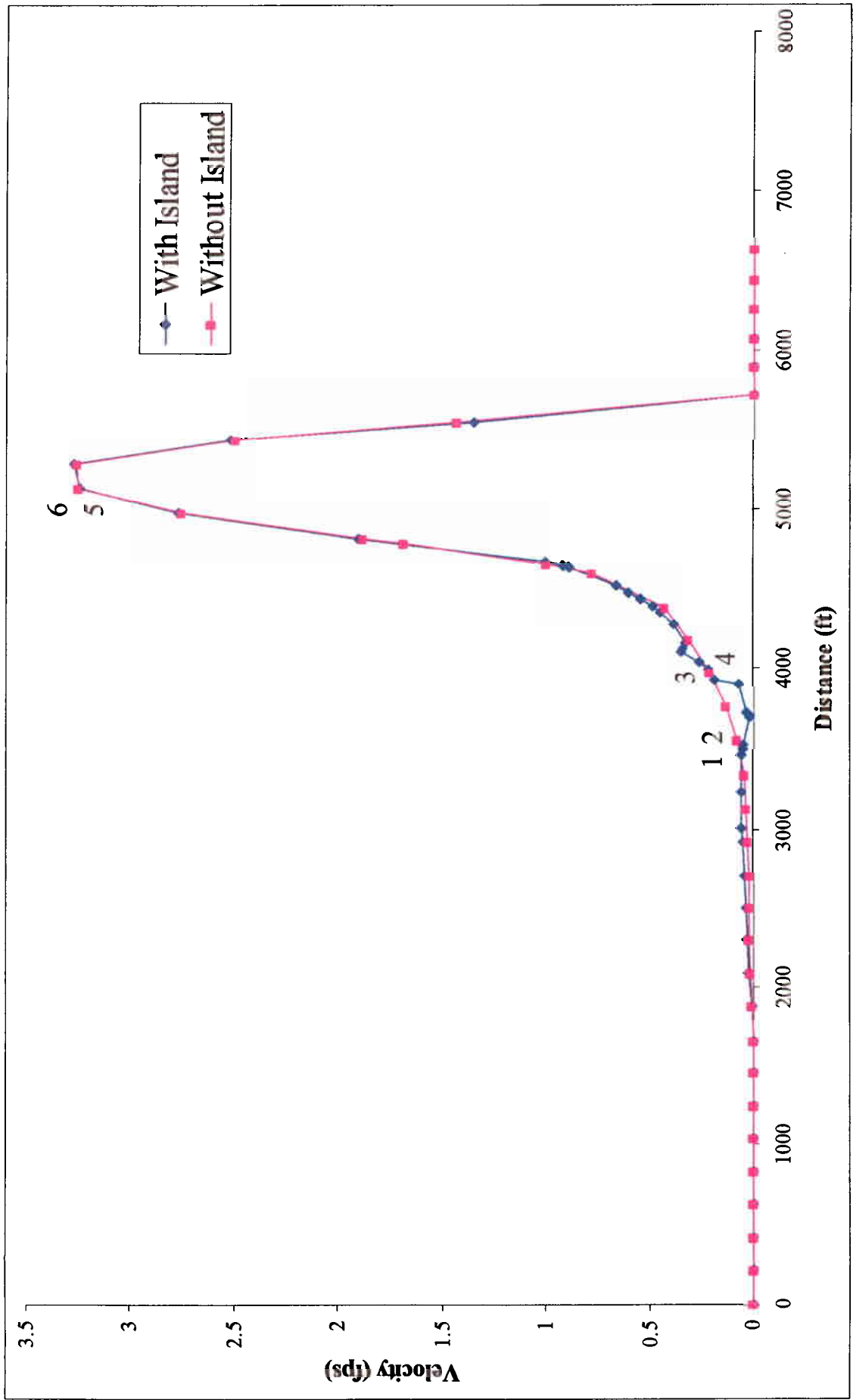


Figure 10. Lateral Velocity Distribution at Cross-Section 1, Alternative 1, for a flow of 45,000 cfs

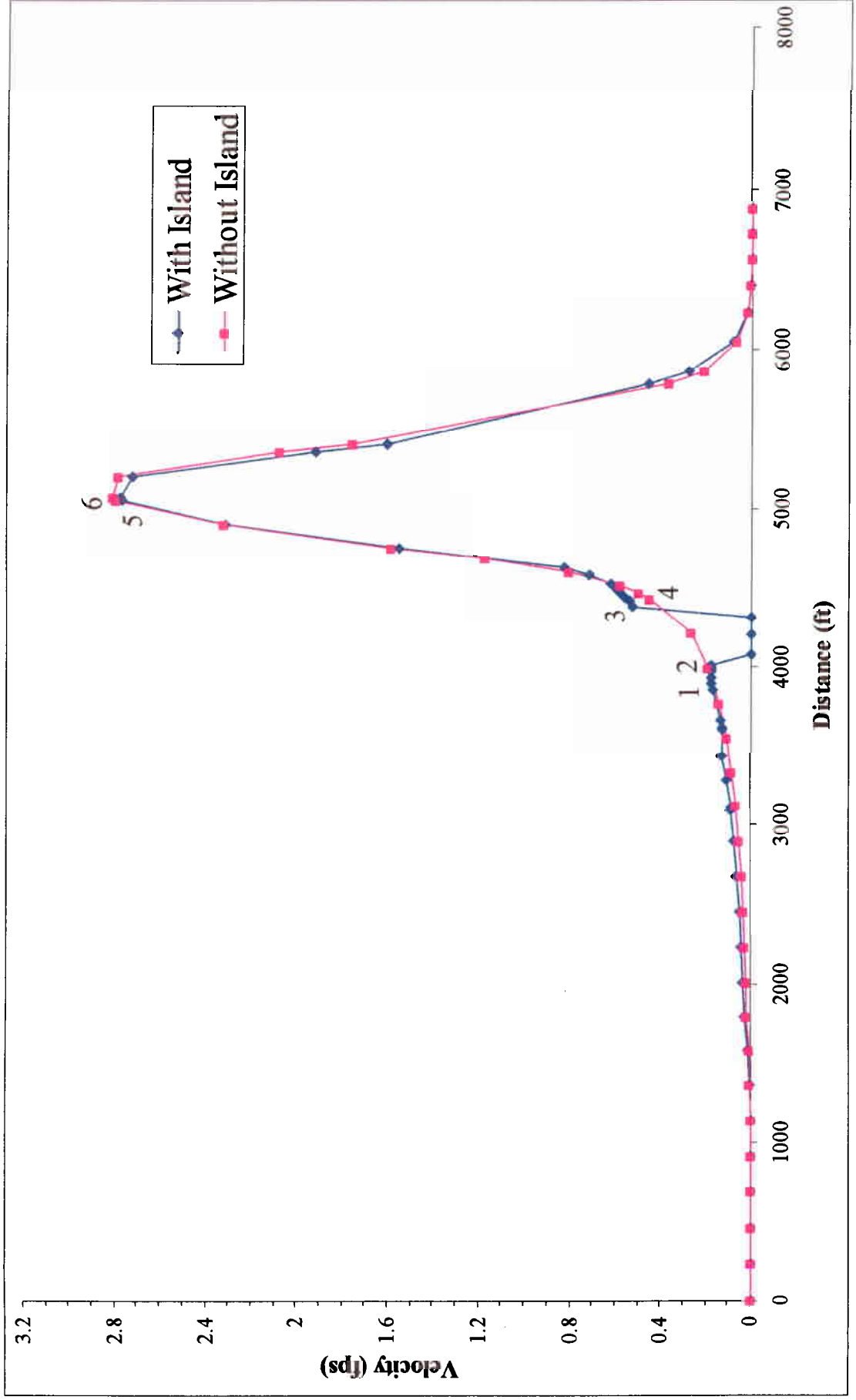


Figure 11. Lateral Velocity Distribution at Cross-Section 2, Alternative 1, for a flow of 45,000 cfs

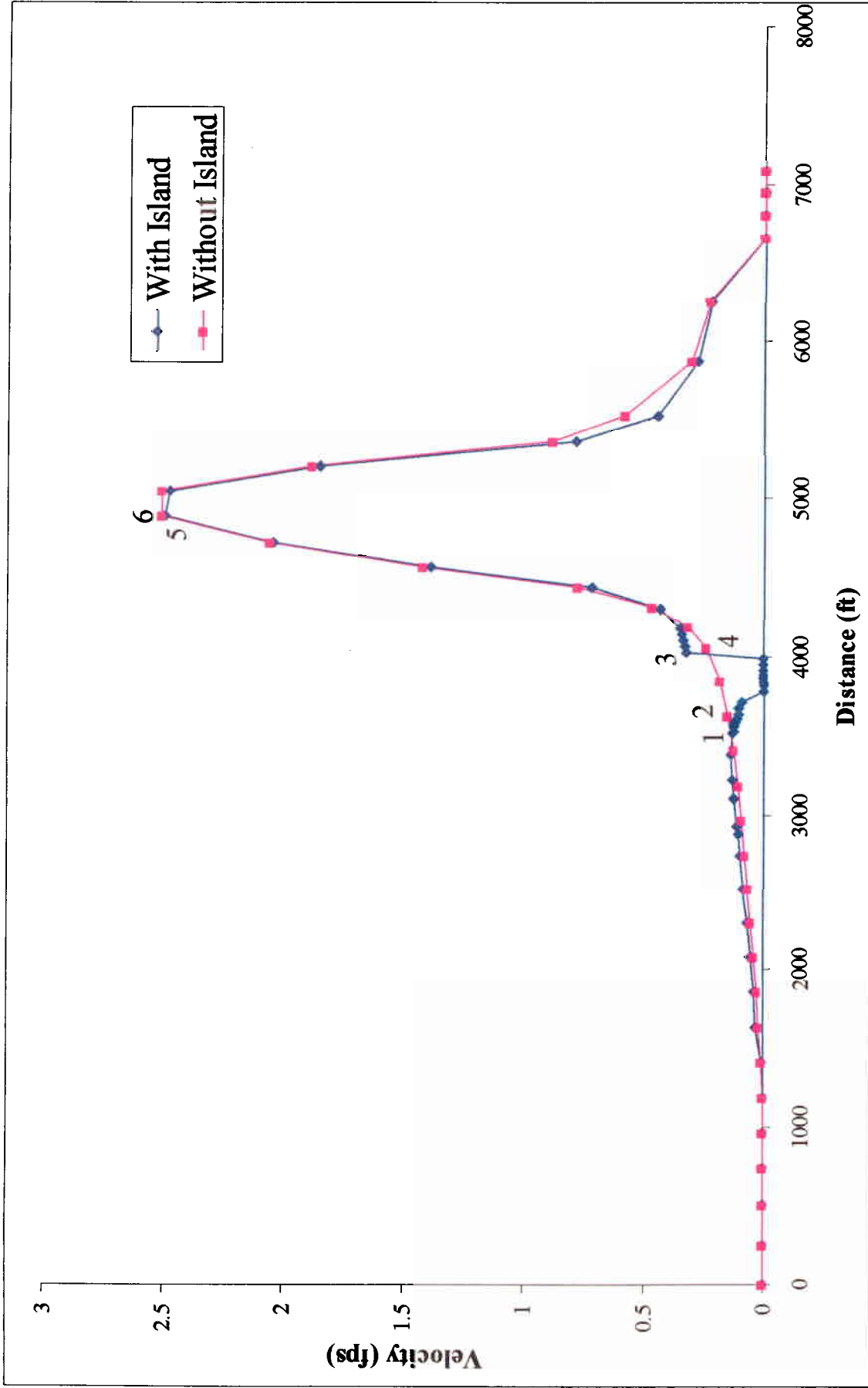


Figure 12. Lateral Velocity Distribution at Cross-Section 3, Alternative 1, for a flow of 45,000 cfs

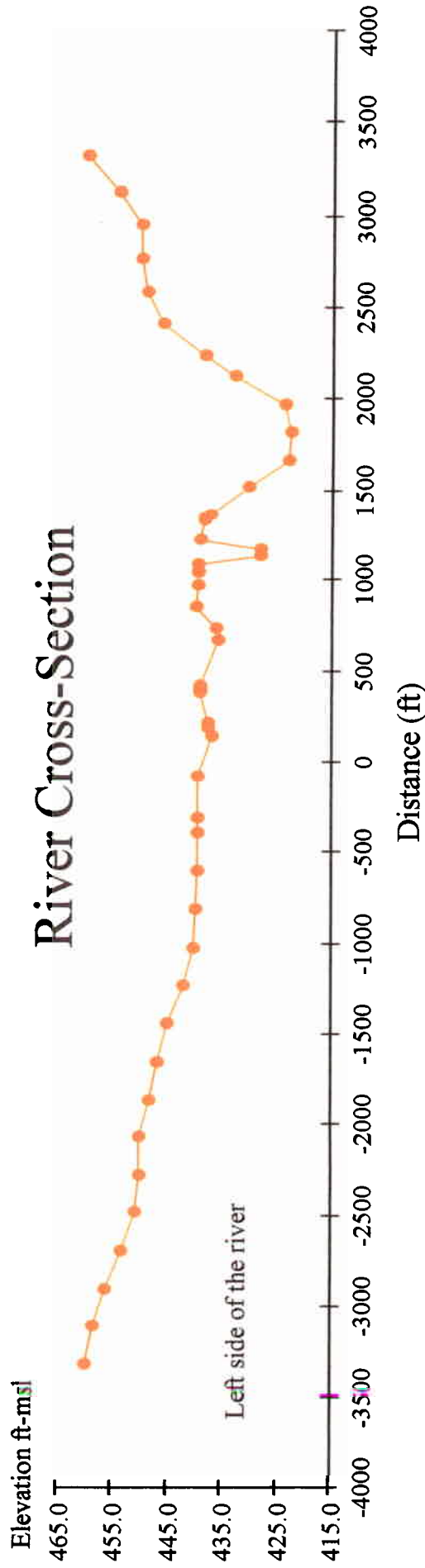
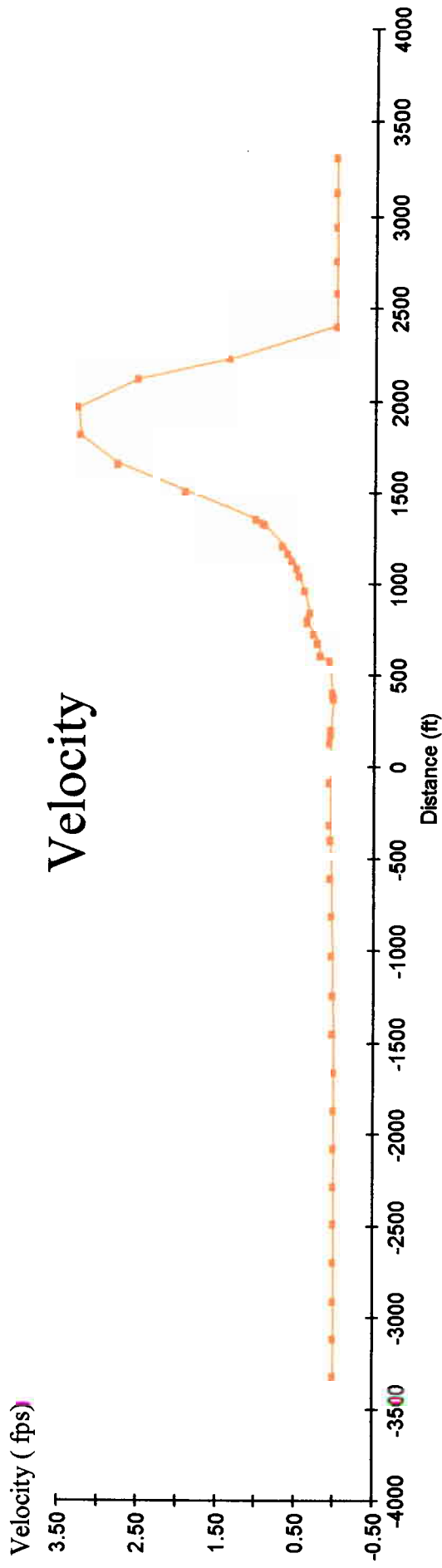


Figure 13. Lateral Velocity Distribution and River Cross-Section at Cross-Section 1, Alternative 1, for a flow of 45,000 cfs

# Velocity

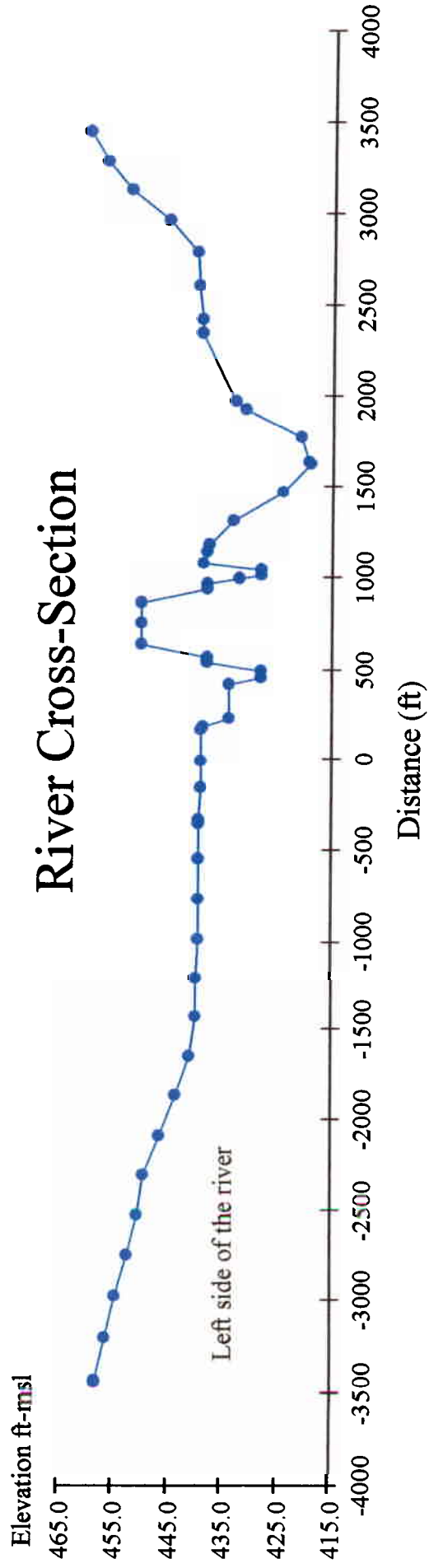
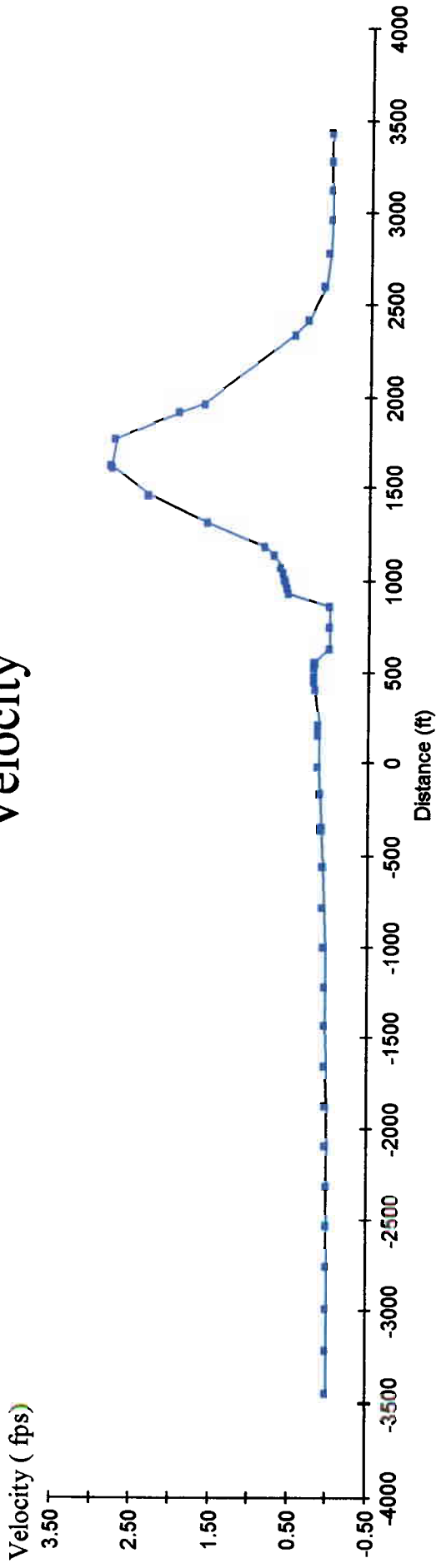


Figure 14. Lateral Velocity Distribution and River Cross-Section at Cross-Section 2, Alternative 1, for a flow of 45,000 cfs

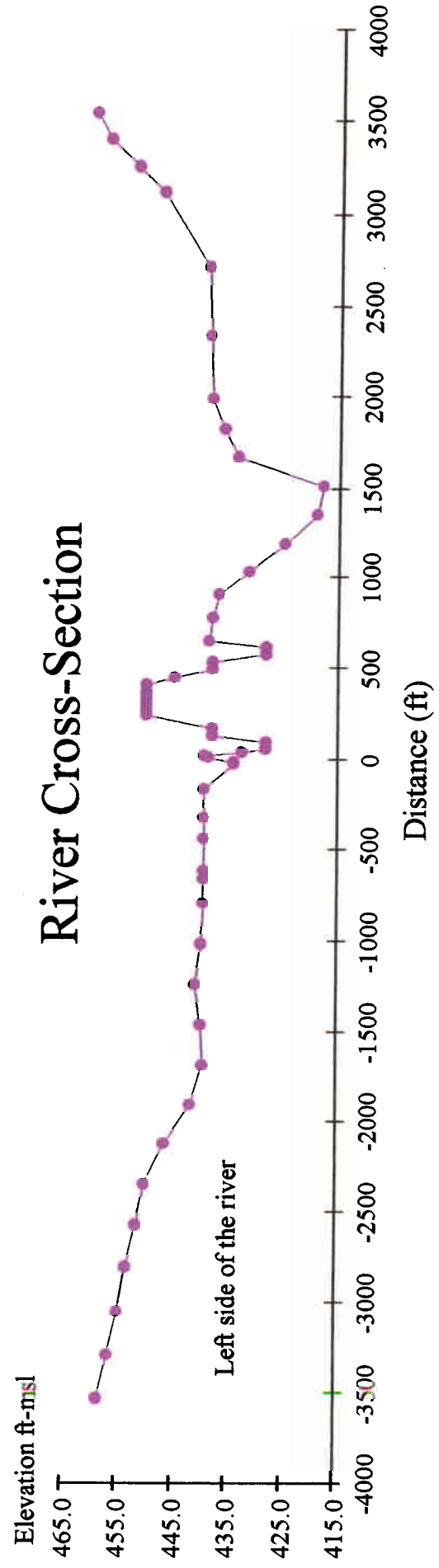
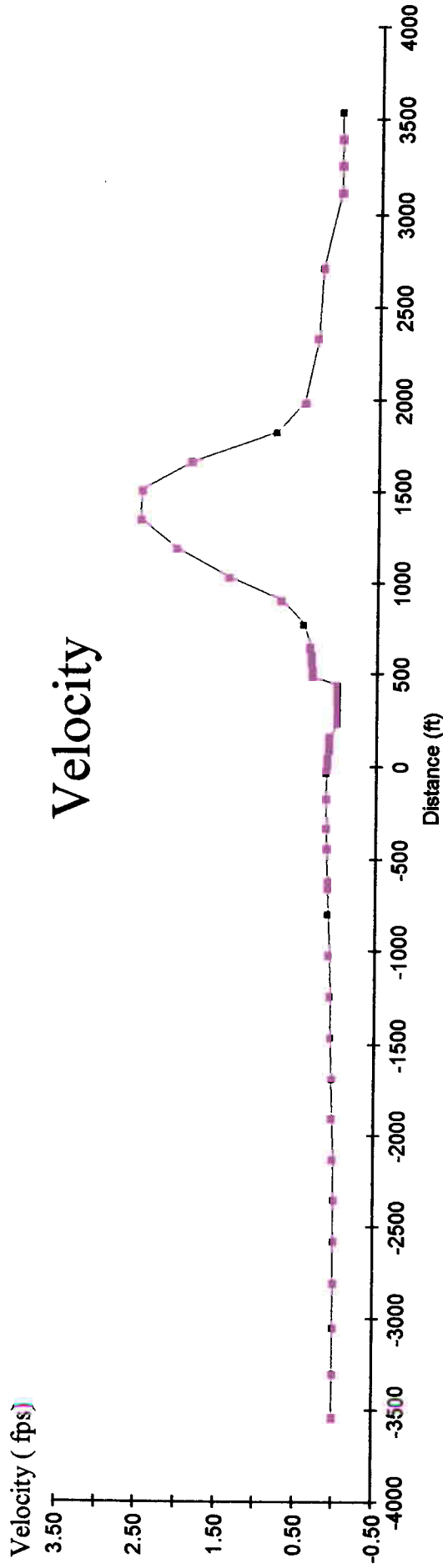


Figure 15. Lateral Velocity Distribution and River Cross-Section at Cross-Section 3, Alternative 1, for a flow of 45,000 cfs

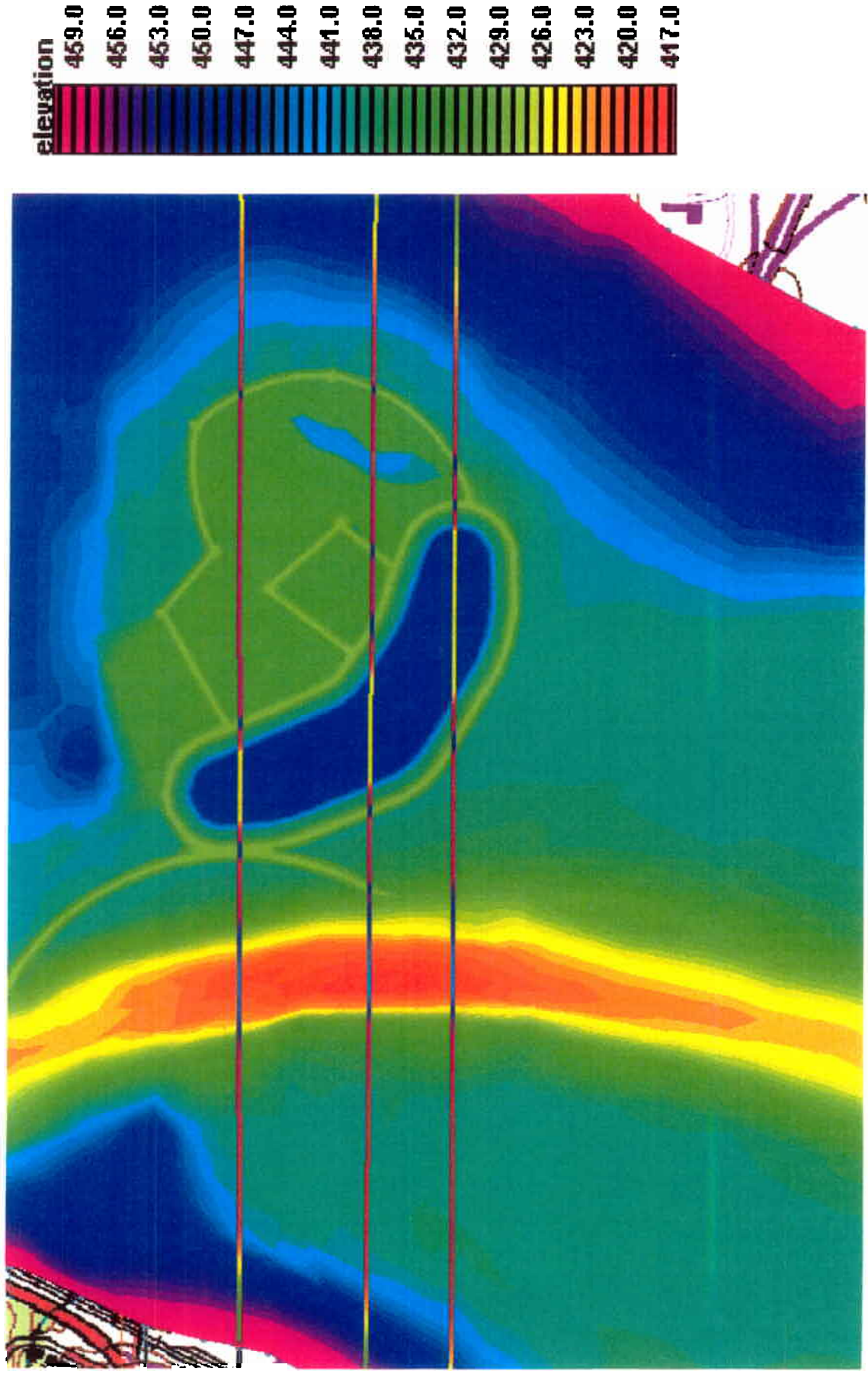


Figure 16. Planform and the Depth Variations for Alternative 2

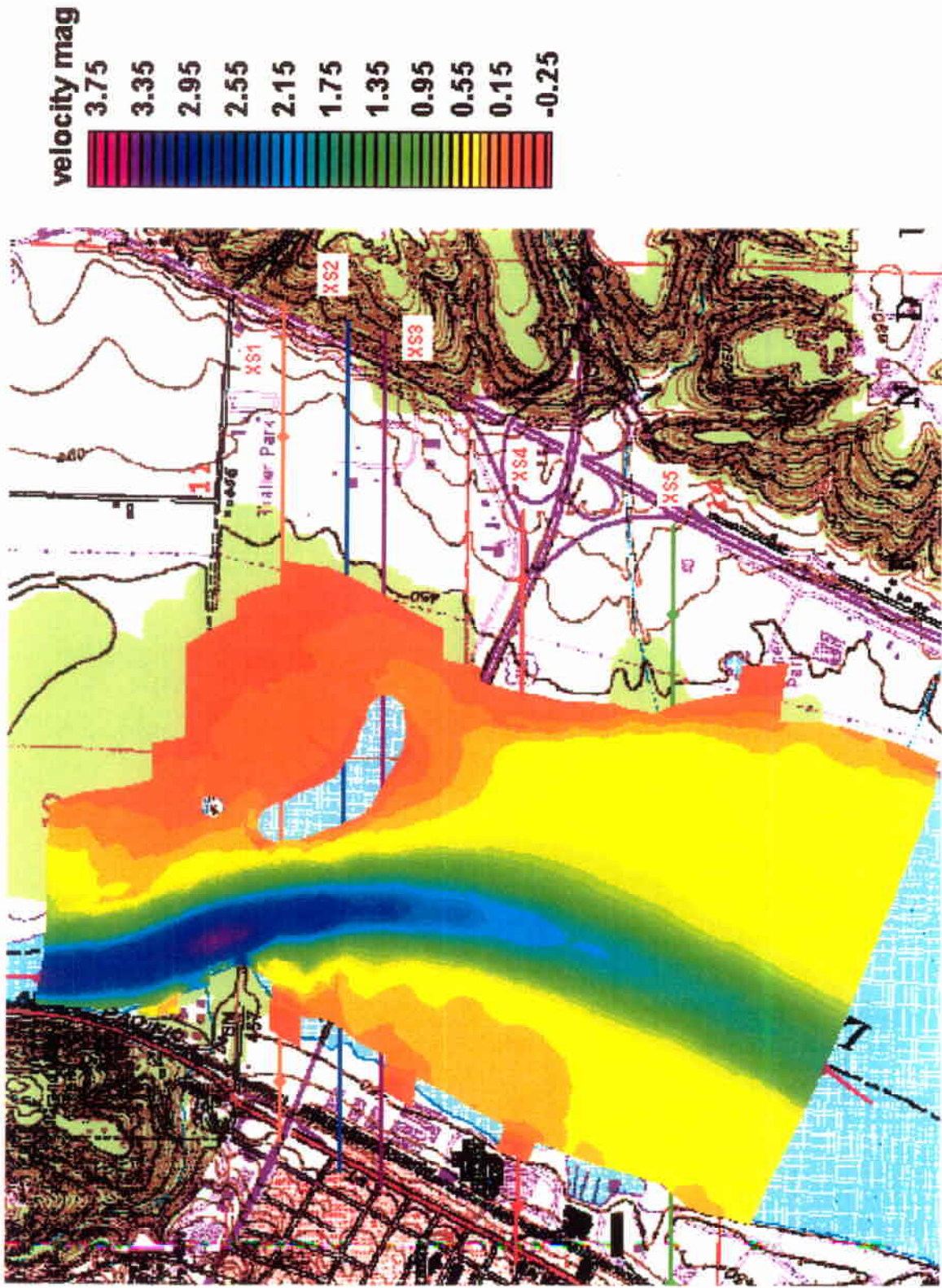


Figure 17. Spatial Velocity Distribution for Alternative 2, for a flow of 45,000 cfs

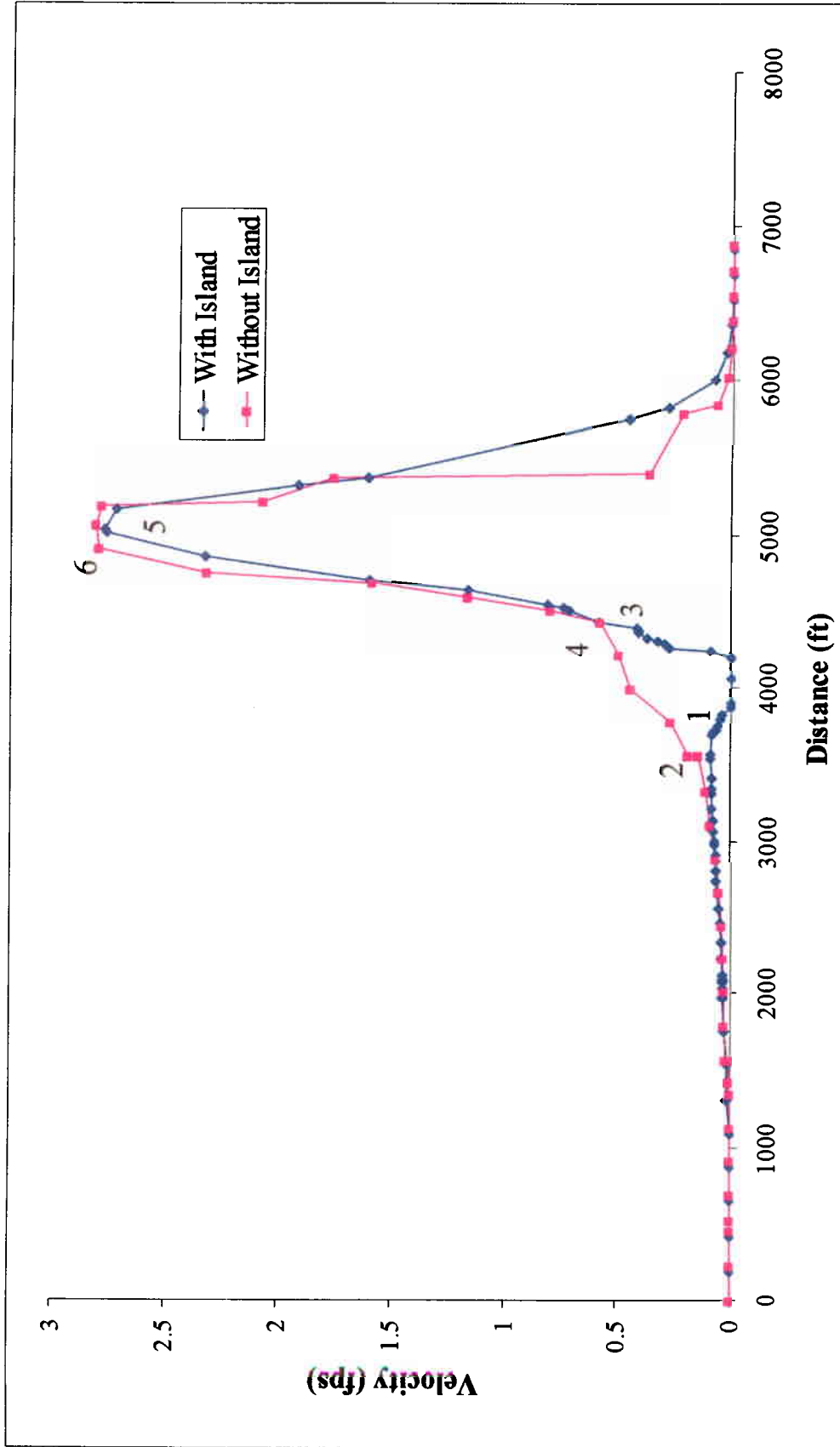


Figure 18. Lateral Velocity Distribution at Cross-Section 1 for Alternative 2, for a flow of 45,000 cfs

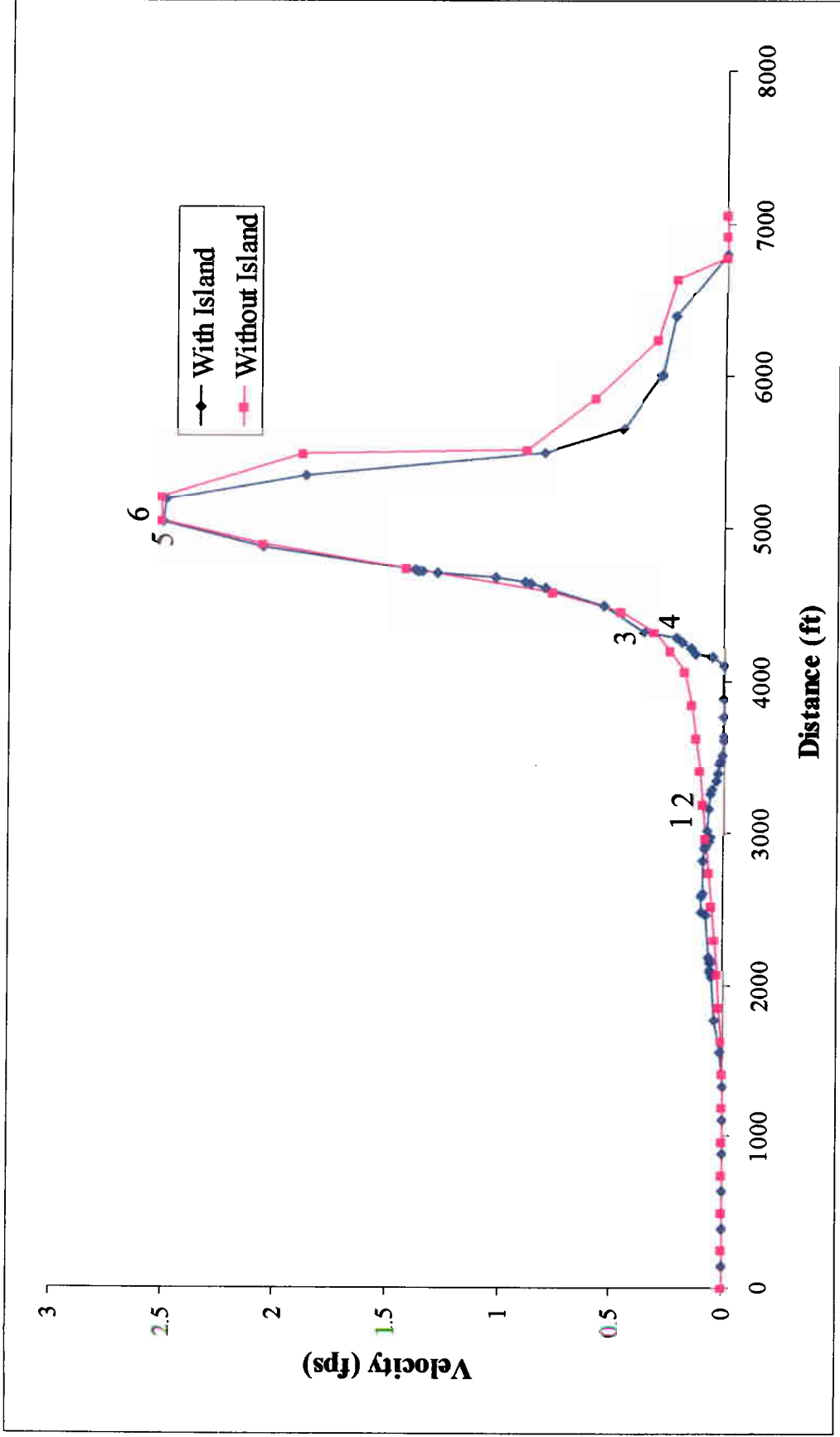


Figure 19. Lateral Velocity Distribution at Cross-Section 2 for Alternative 2, for a flow of 45,000 cfs

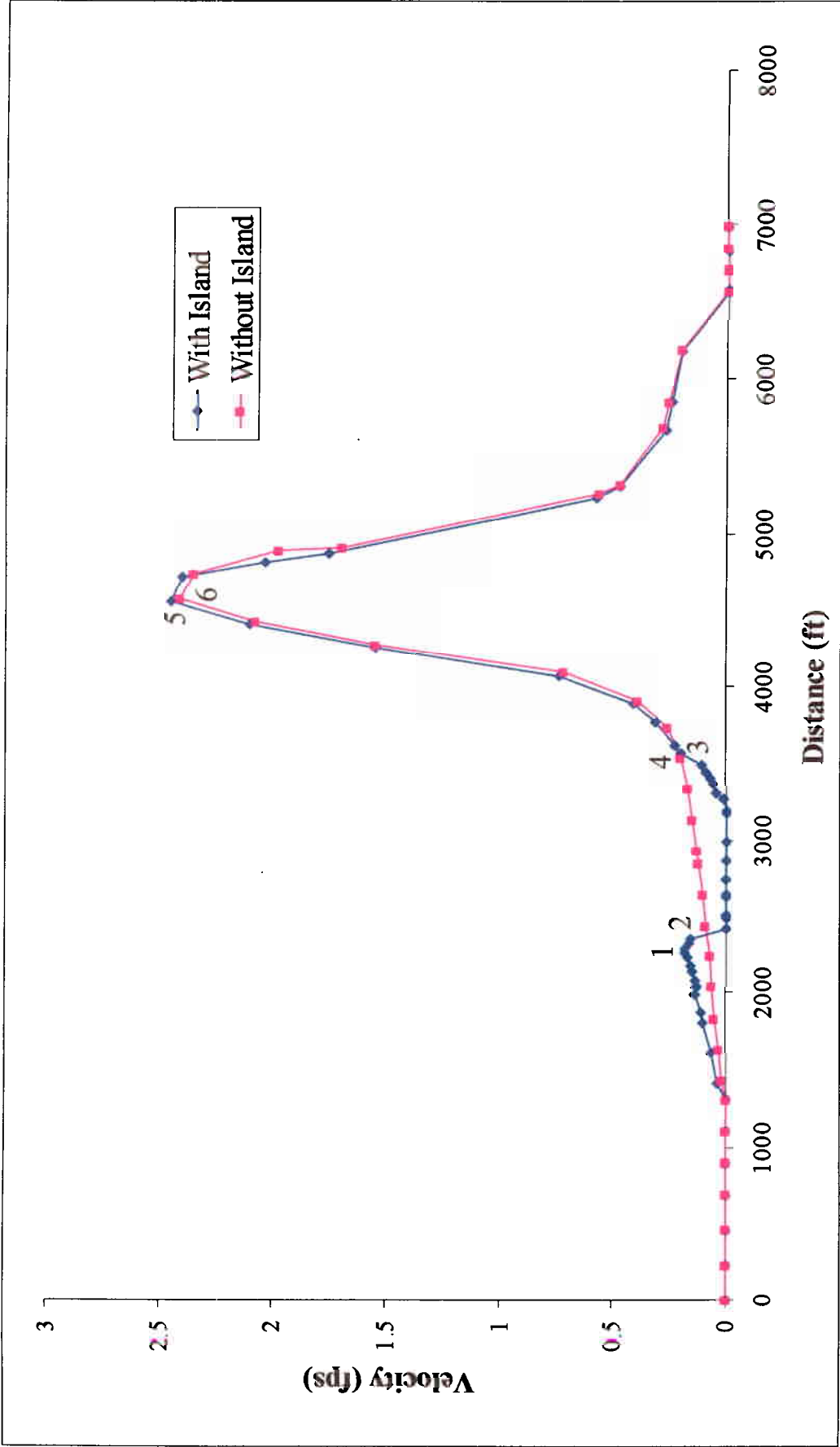


Figure 20. Lateral Velocity Distribution at Cross-Section 3 for Alternative 2, for a flow of 45,000 cfs

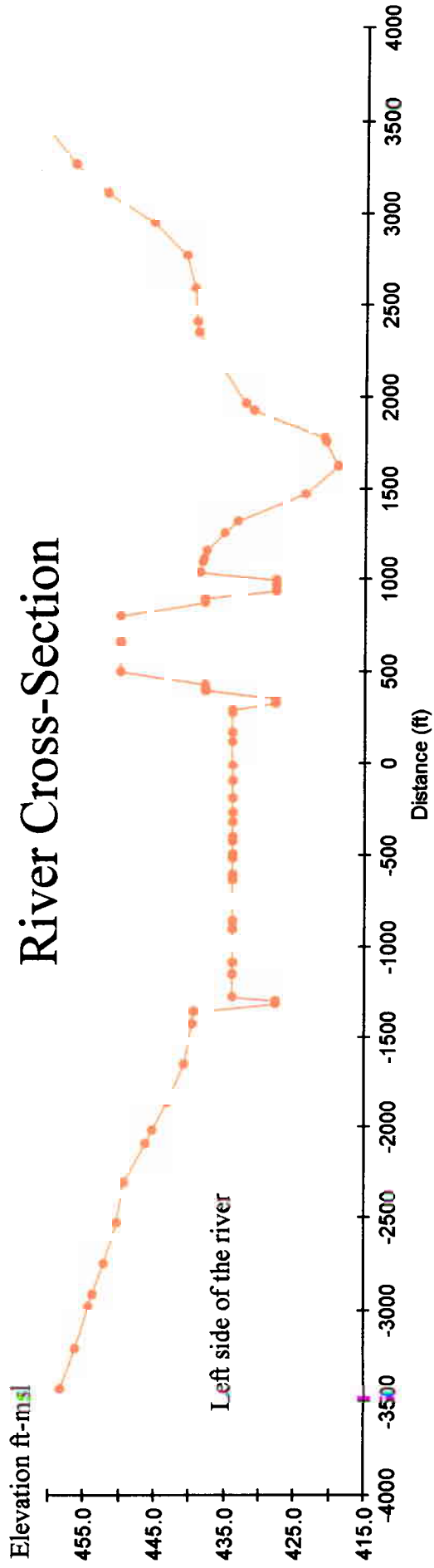
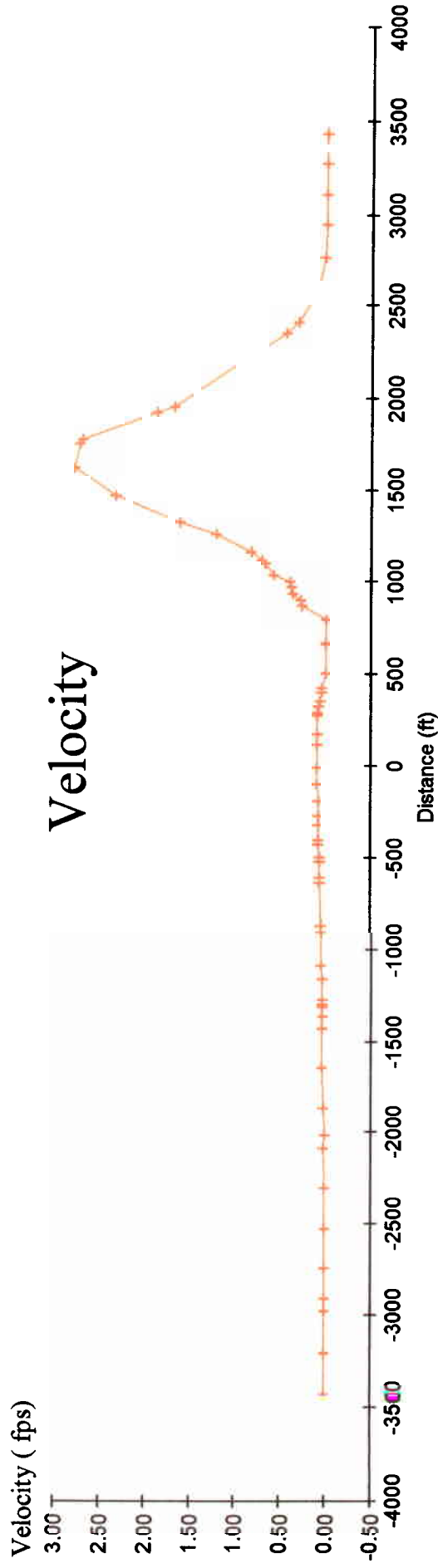


Figure 21. Lateral Velocity Distribution and River Cross-Section at Cross-Section 1 for Alternative 2, for a flow of 45,000 cfs

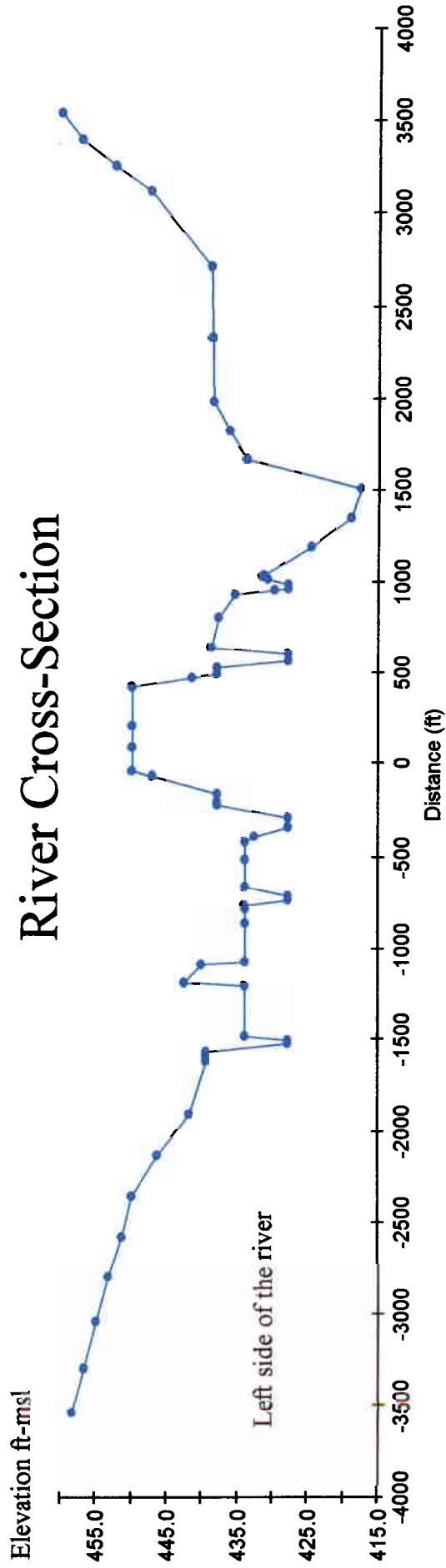
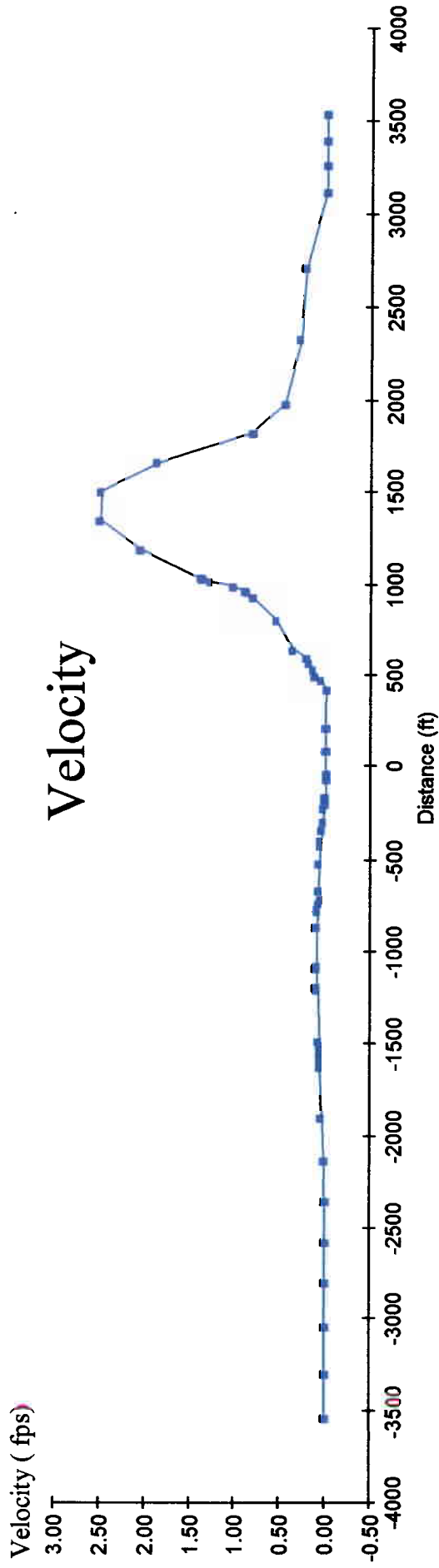


Figure 22. Lateral Velocity Distribution and River Cross-Section at Cross-Section 2 for Alternative 2, for a flow of 45,000 cfs

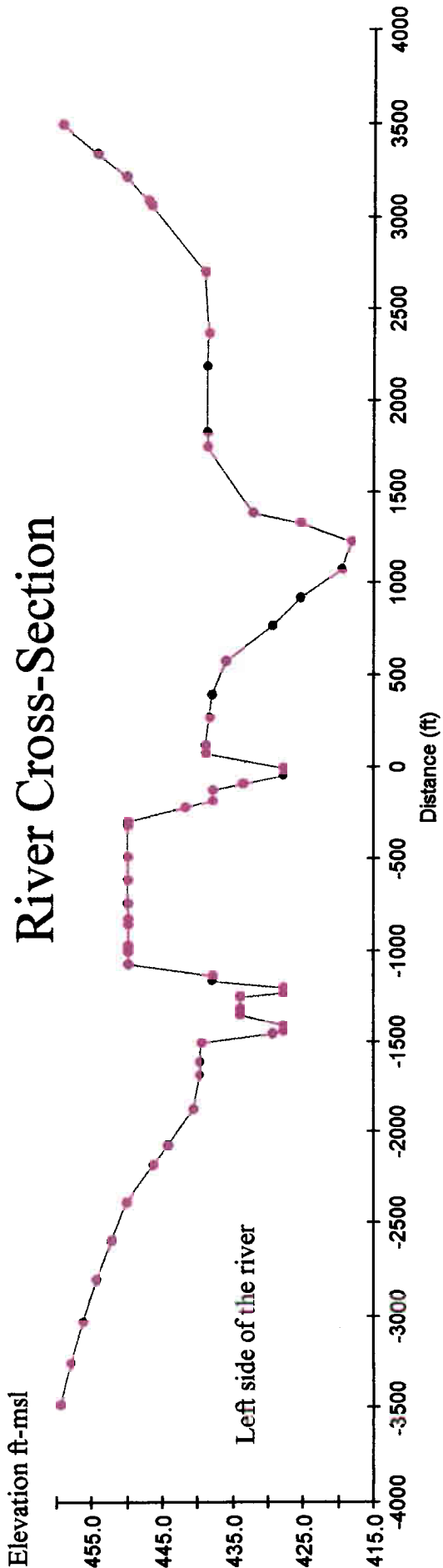
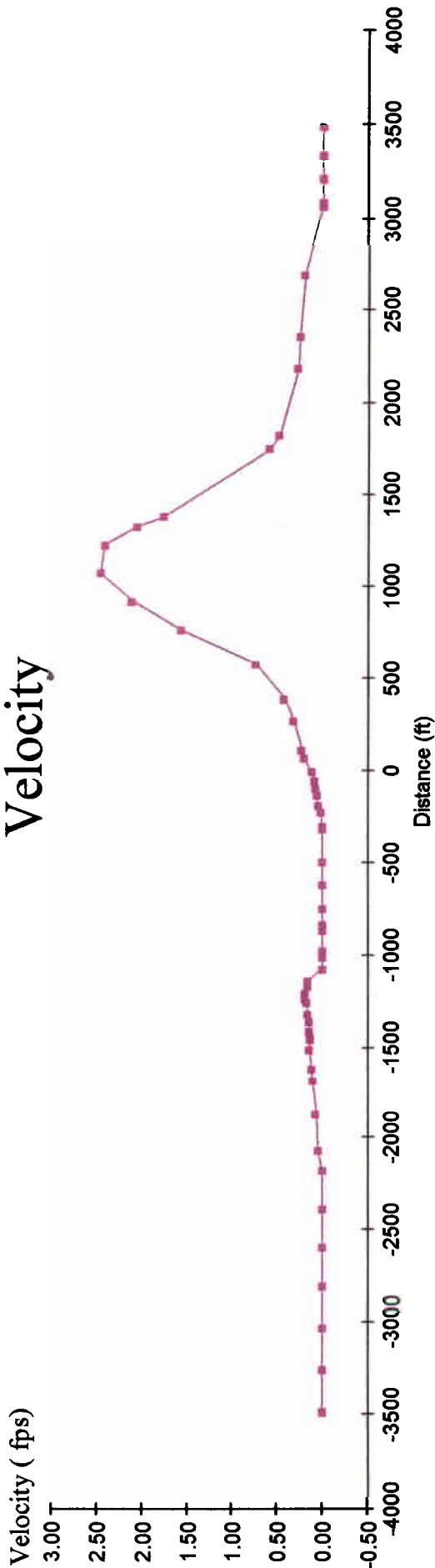


Figure 23. Lateral Velocity Distribution and River Cross-Section at Cross-Section 3 for Alternative 2, for a flow of 45,000 cfs

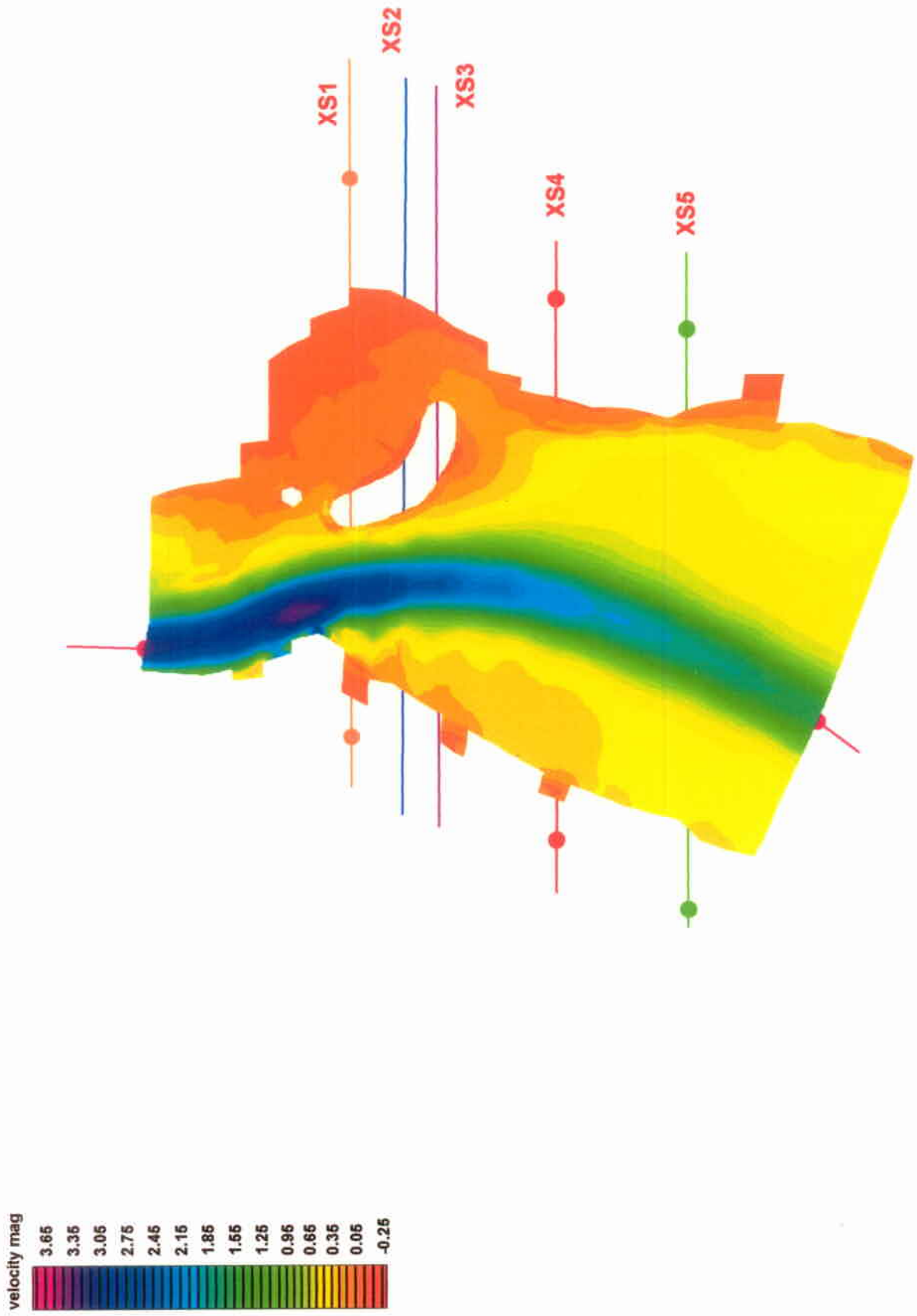


Figure 24. Location of Cross-Sections for Alternative 2

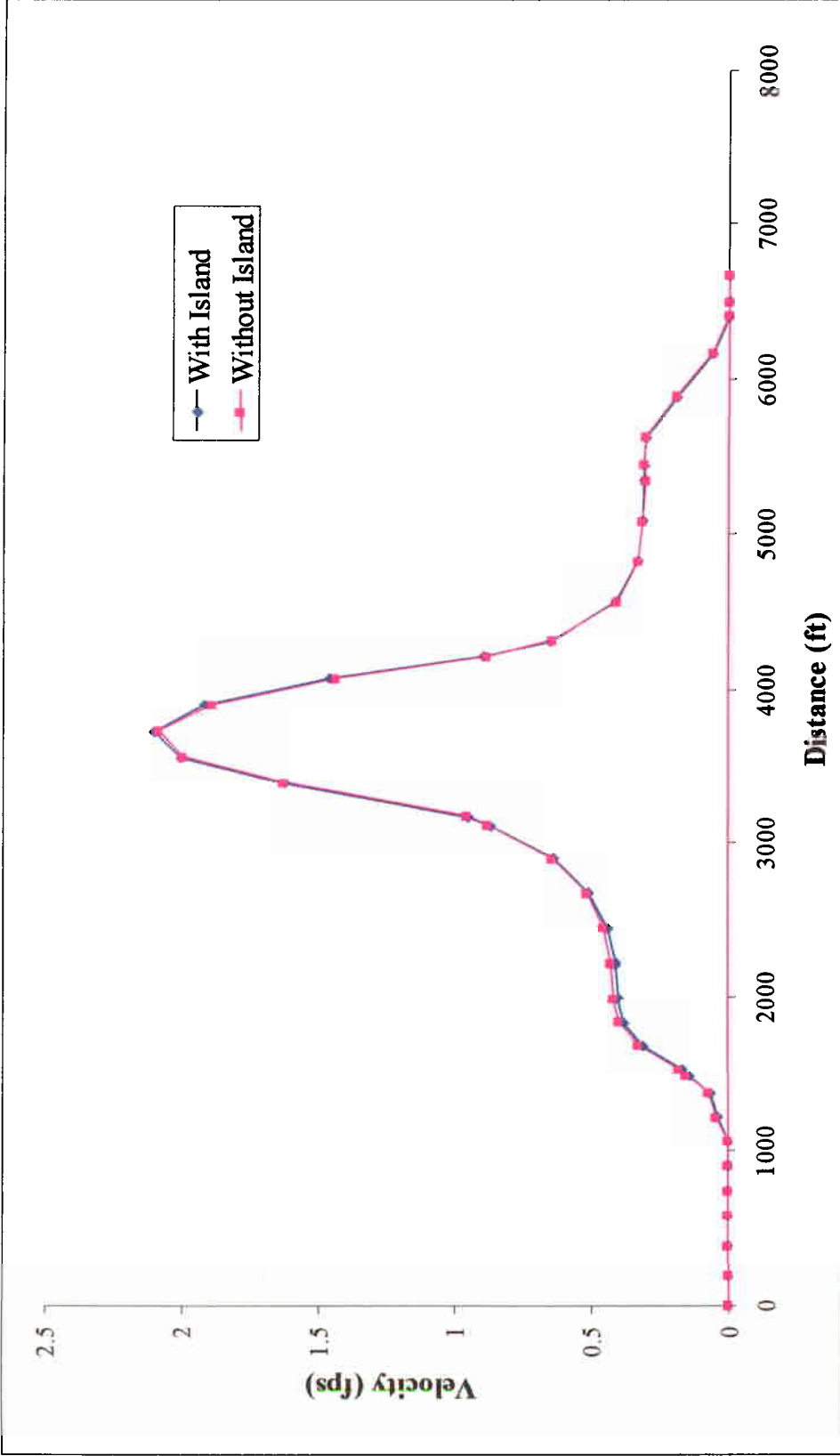


Figure 25. Lateral Velocity Distribution at Cross-Section 4 Below McClugge Bridge for Alternative 2, for a flow of 45,000 cfs

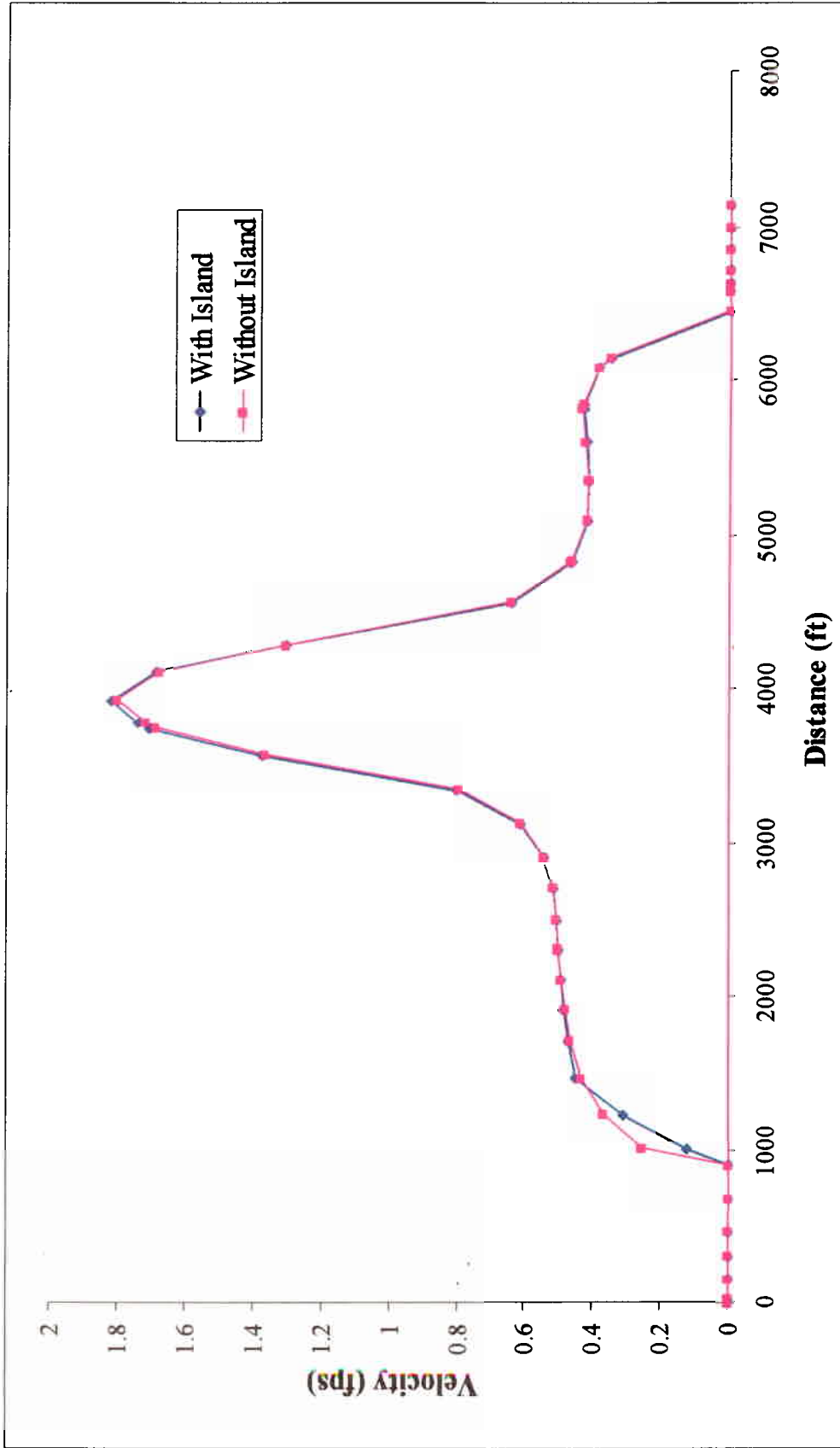


Figure 26. Lateral Velocity Distribution at Cross-Section 5 Below McClugge Bridge for Alternative 2, for a flow of 45,000 cfs

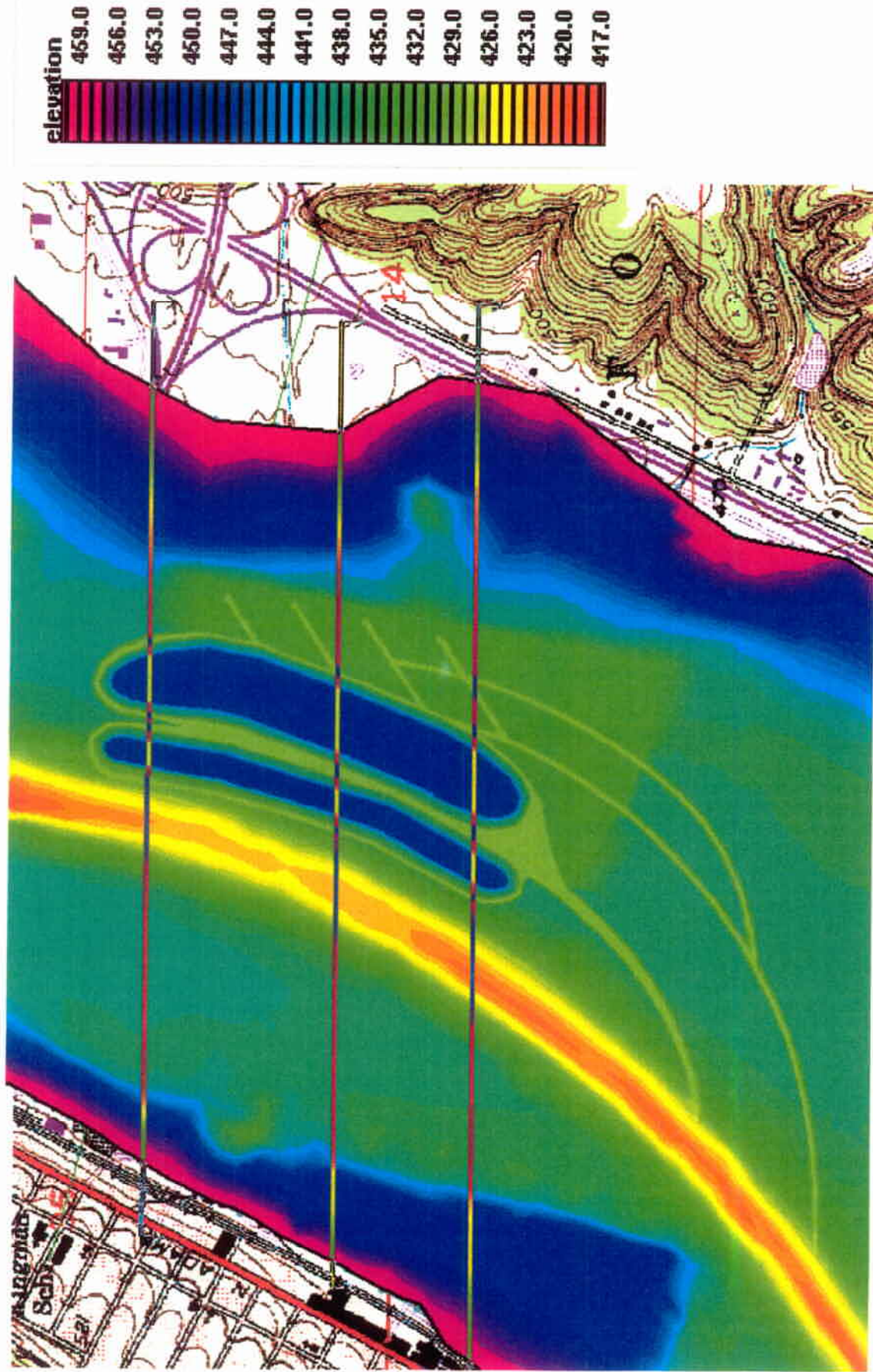


Figure 27. Depth Variations for Alternative 3 Including the Locations of the Potential Dredged Channels

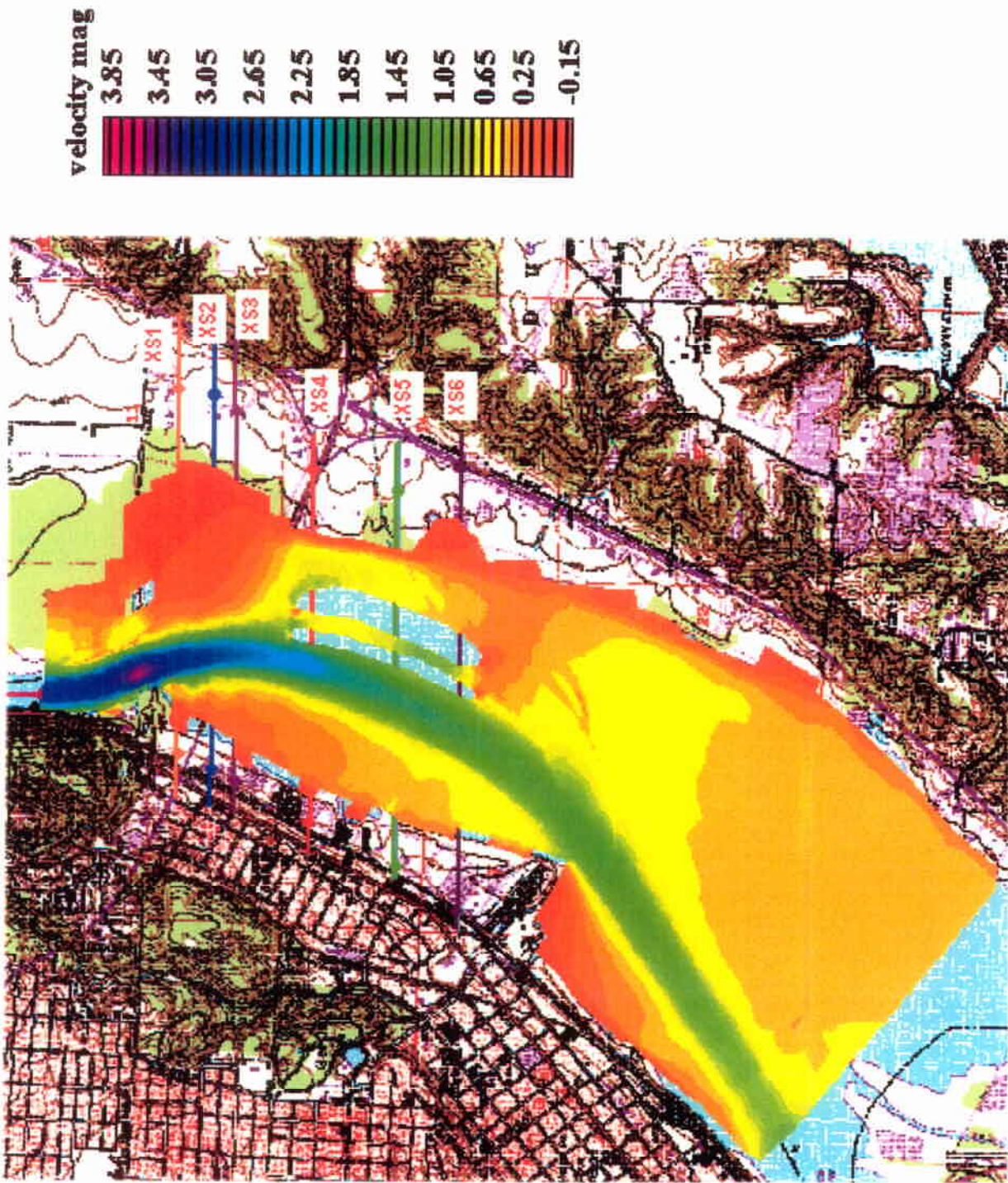


Figure 28. Spatial Velocity Distribution for Alternative 3, for a flow of 45,000 cfs

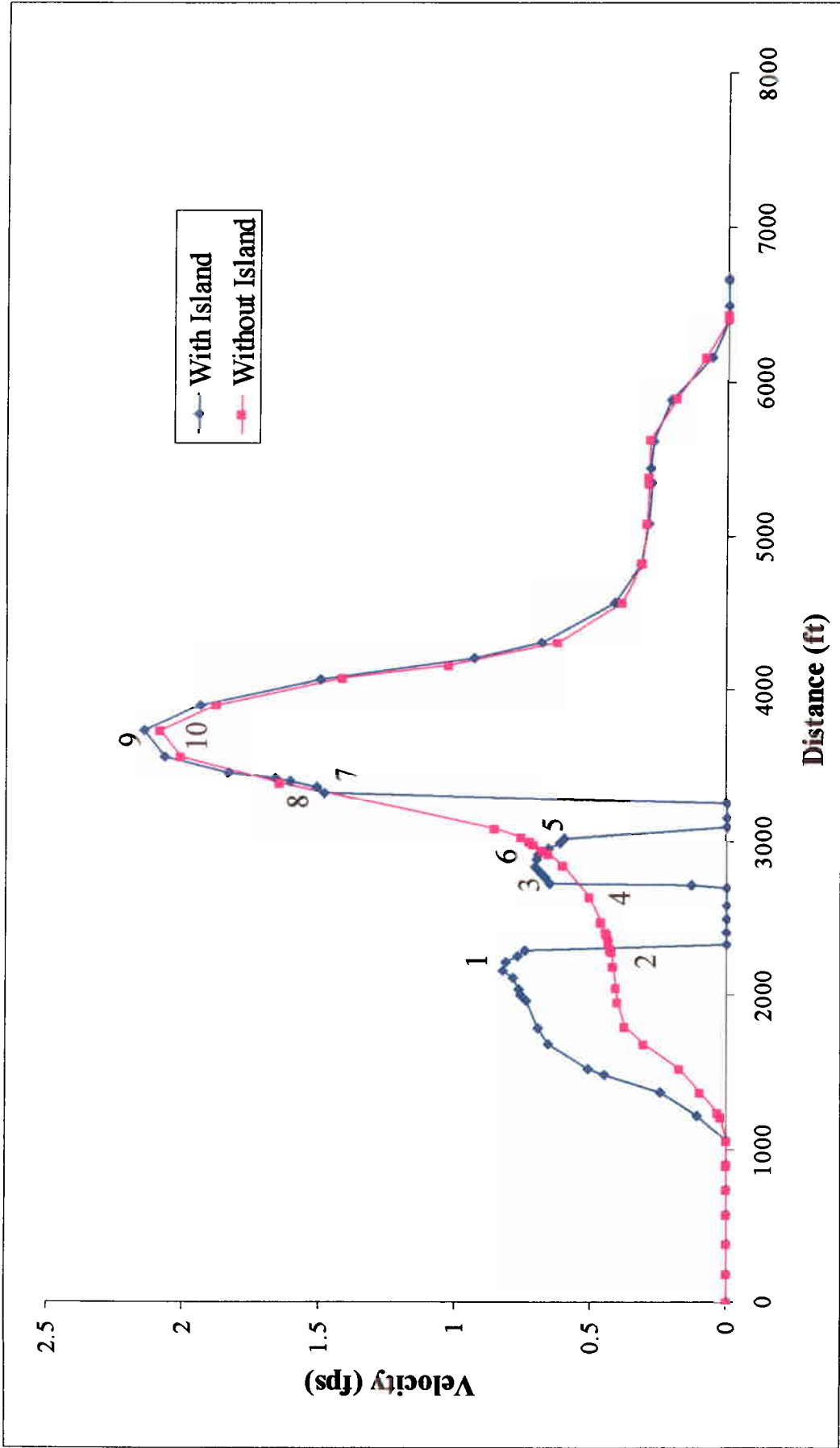


Figure 29. Lateral Velocity Distributions at Cross-Section 1 for Alternative 3 for a flow of 45,000 cfs

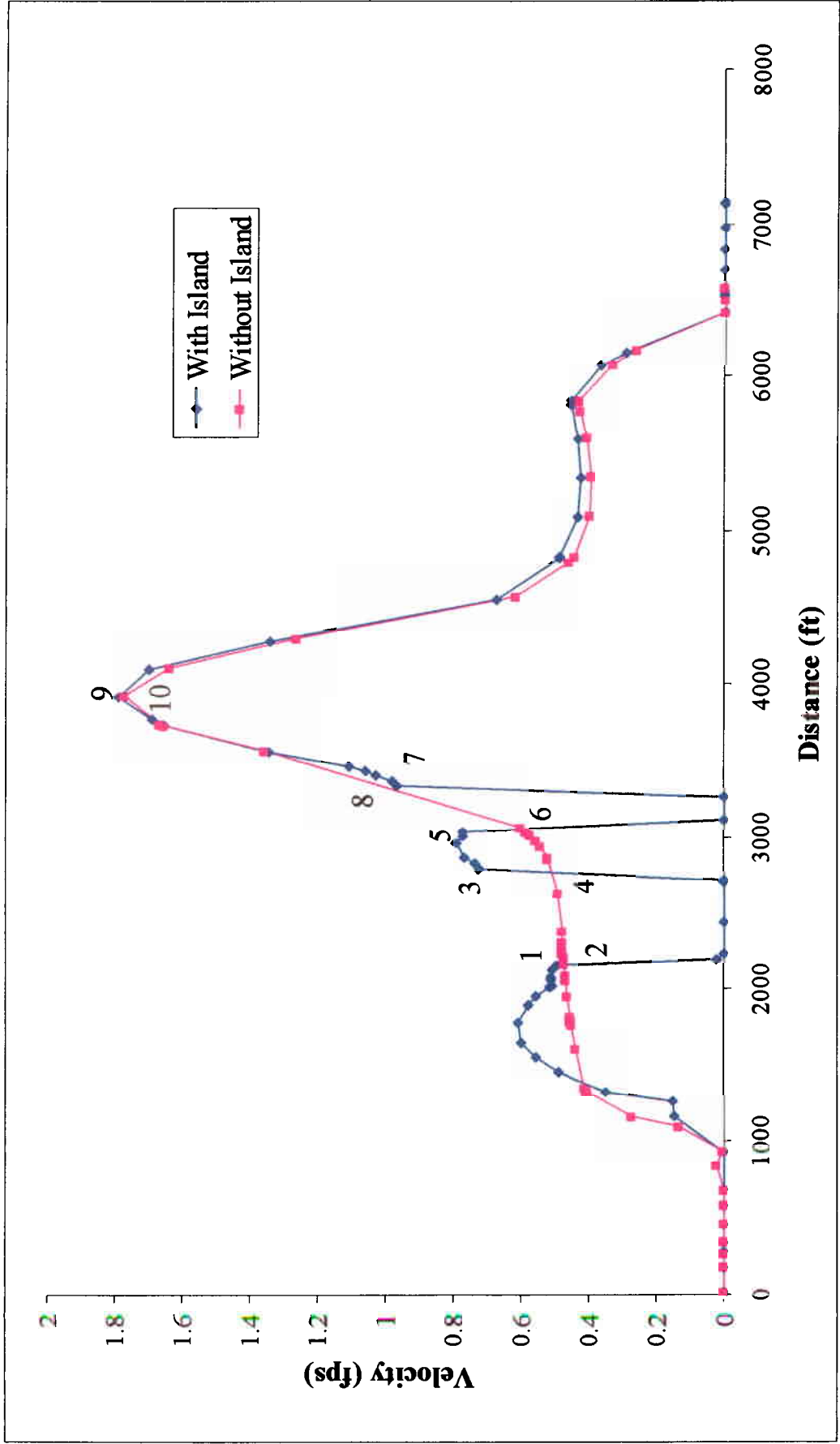


Figure 30. Lateral Velocity Distributions at Cross-Section 2 for Alternative 3 for a flow of 45,000 cfs

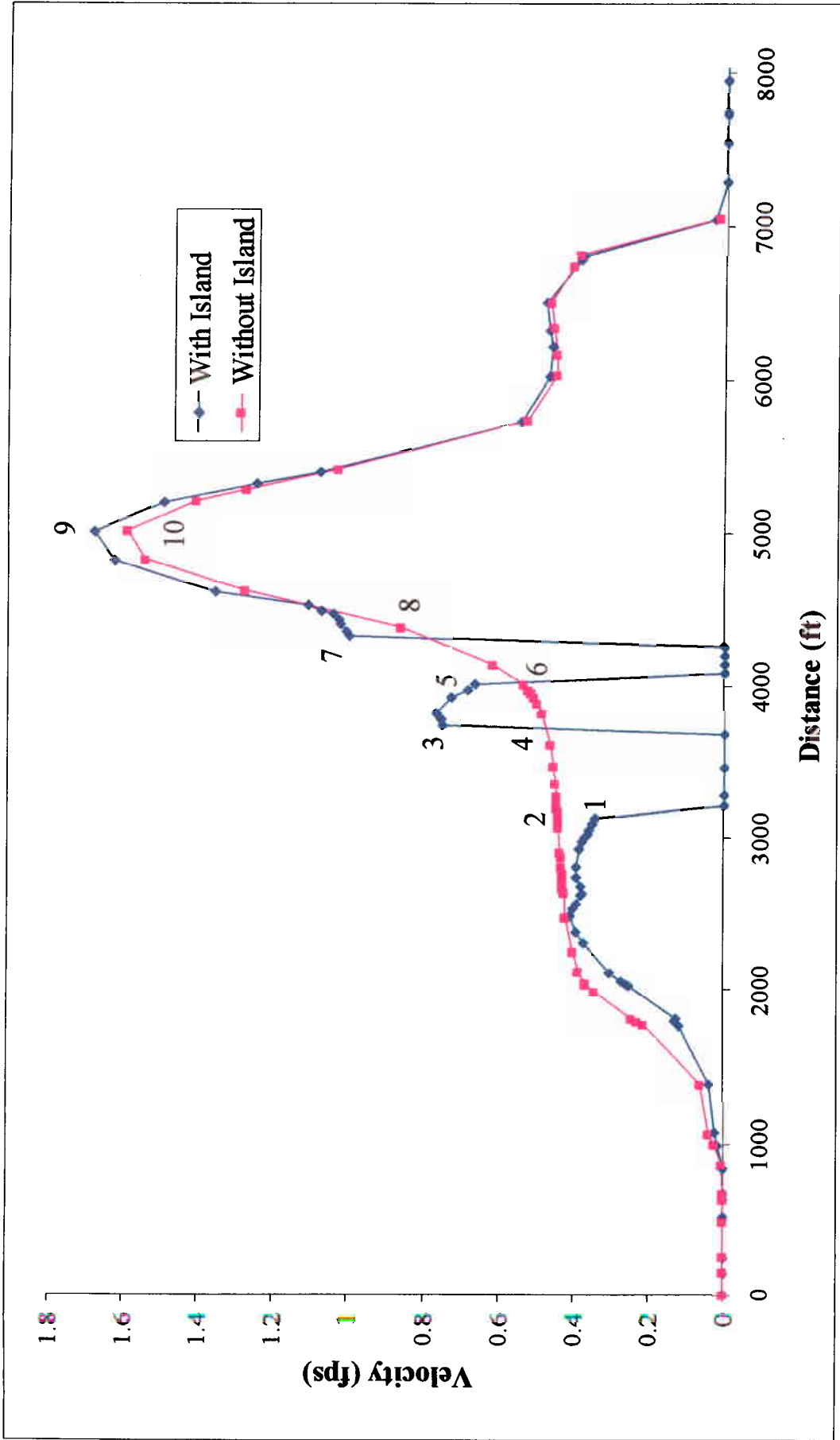


Figure 31. Lateral Velocity Distributions at Cross-Section 3 for Alternative 3 for a flow of 45,000 cfs

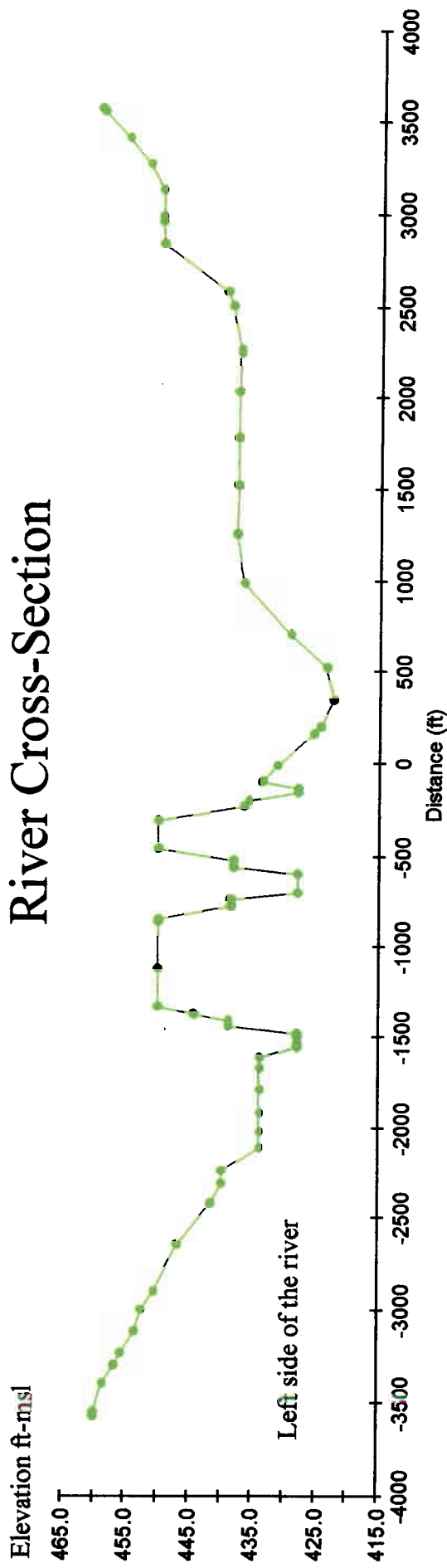
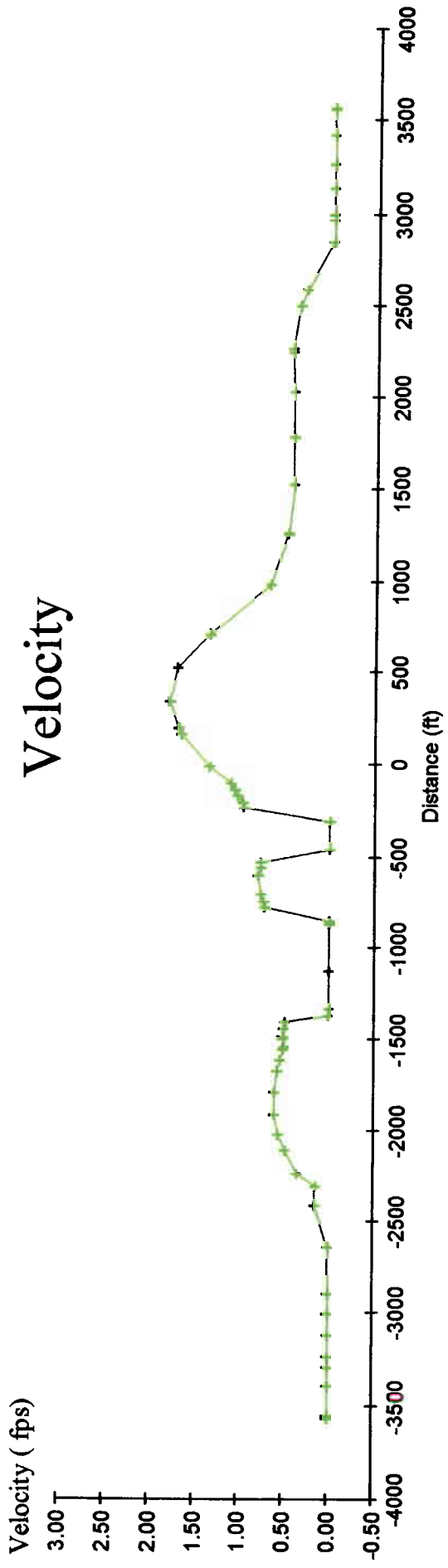


Figure 33. Lateral Velocity Distribution and River Section at Cross-Section 2 for Alternative 3 for a flow of 45,000 cfs

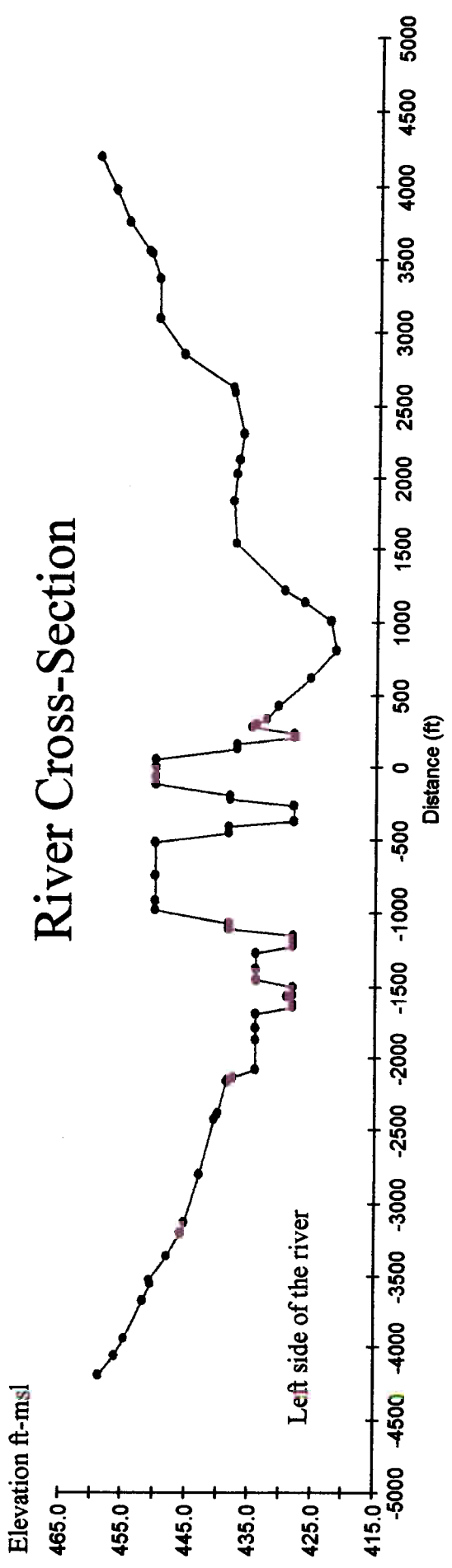
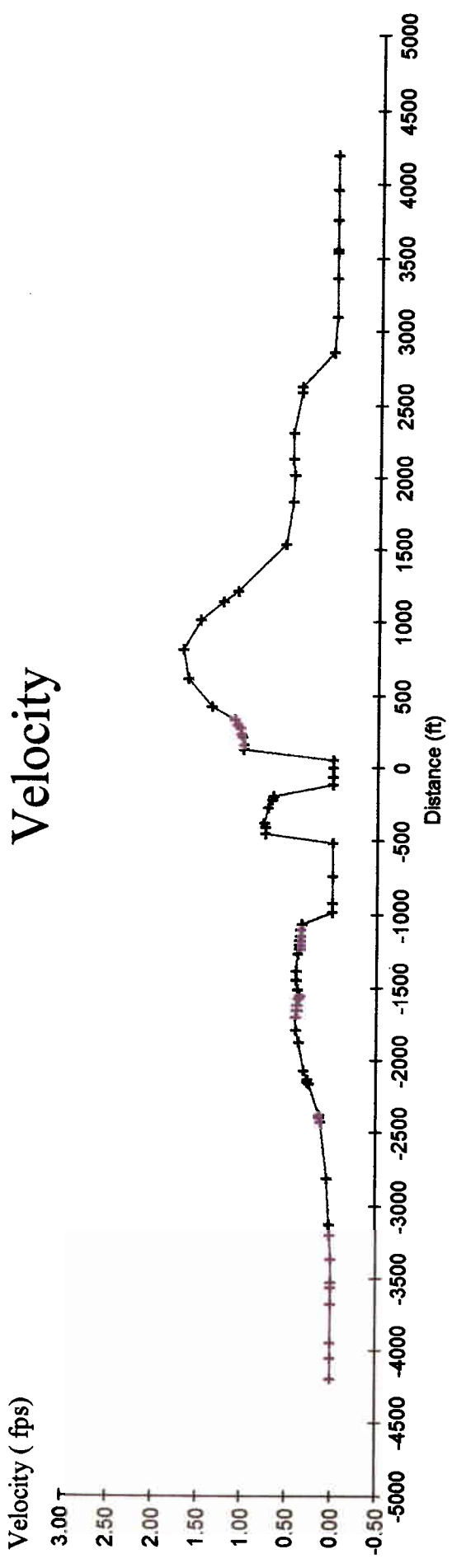


Figure 34. Lateral Velocity Distribution and River Section at Cross-Section 3 for Alternative 3 for a flow of 45,000 cfs

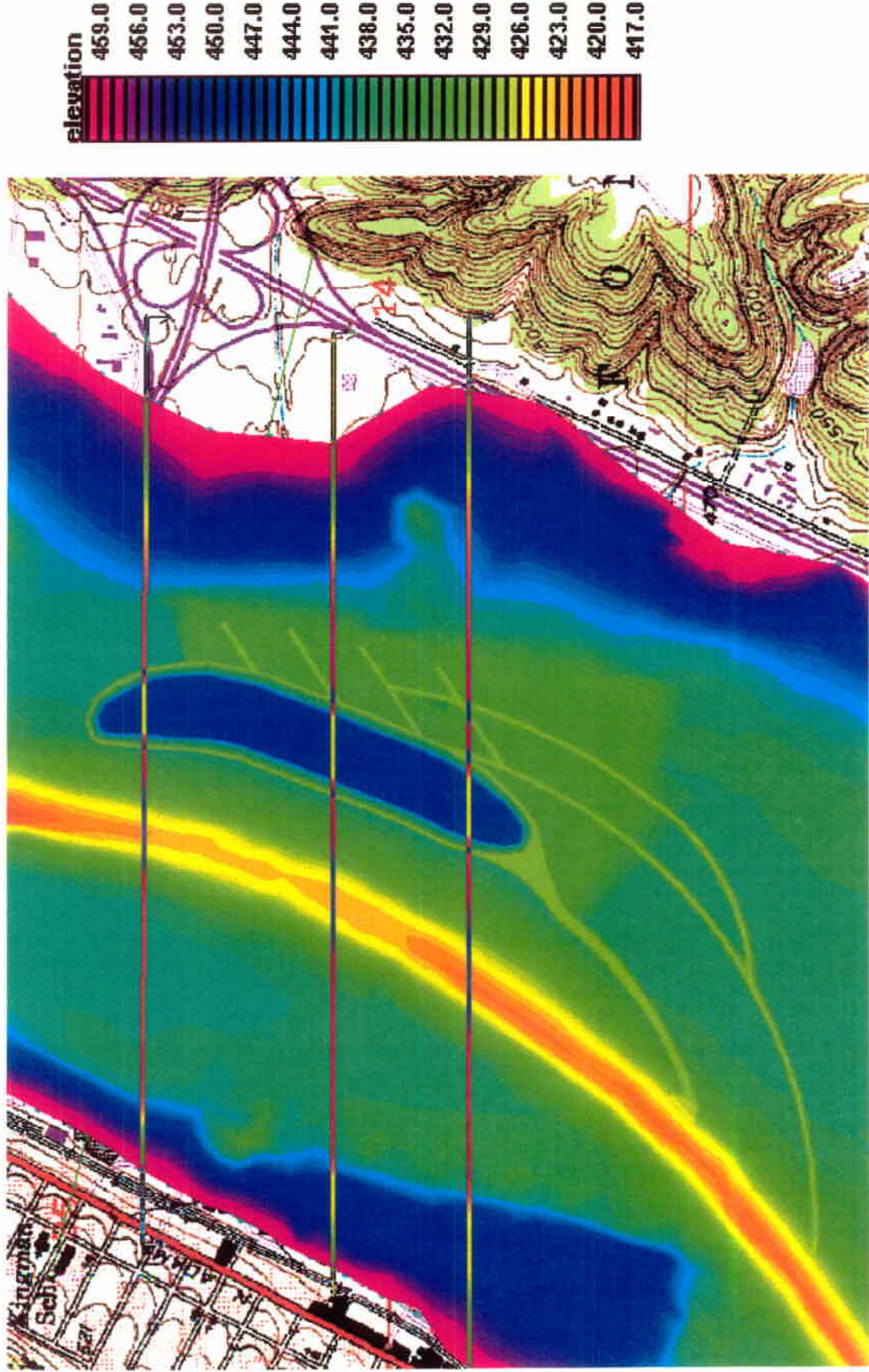


Figure 35. Depth Variations and Dredged Channel Locations for Alternative 4

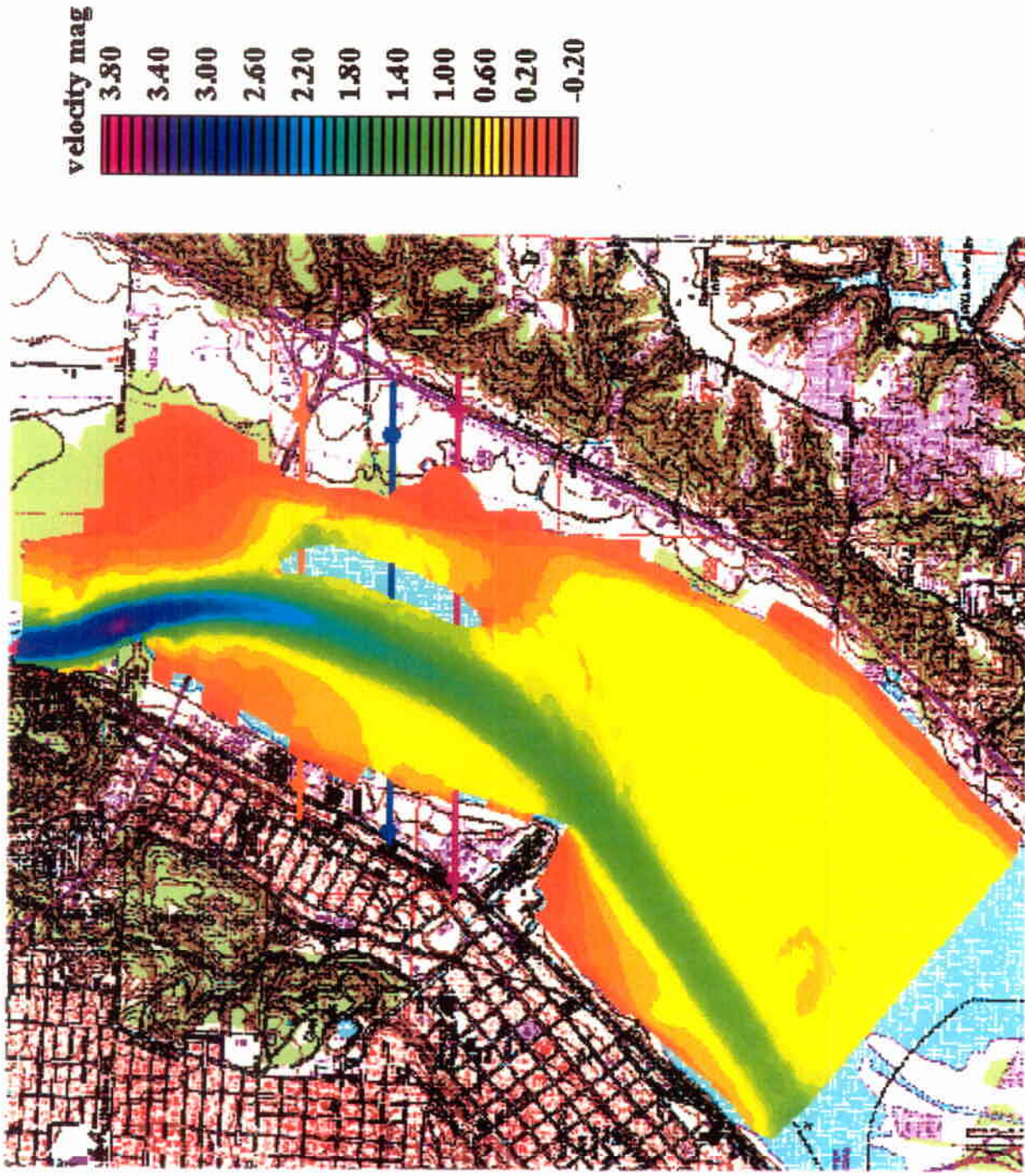


Figure 36. Spatial Velocity Distribution for Alternative 4 for a flow of 45,000 cfs

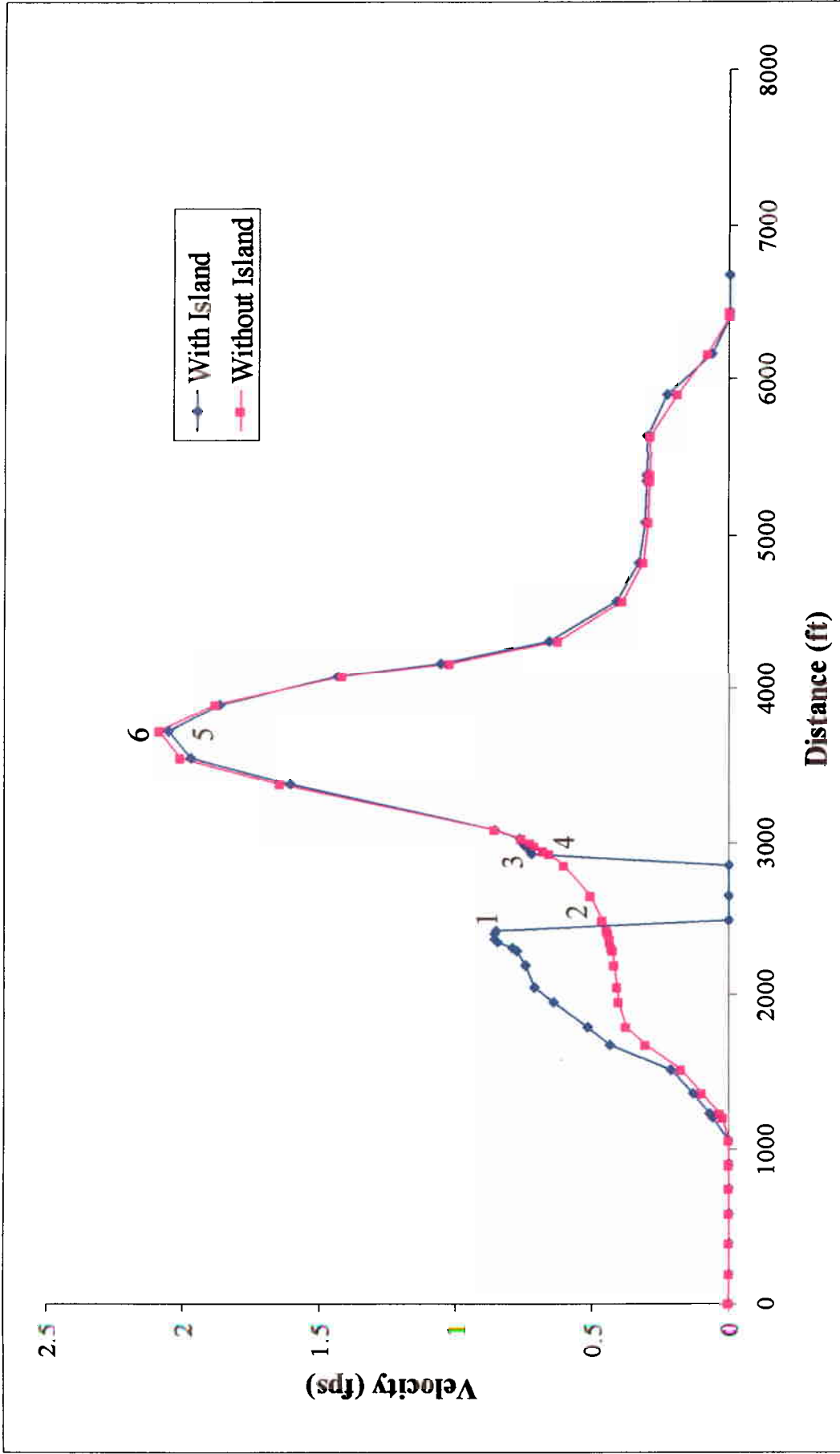


Figure 37. Lateral Velocity Distribution at Cross-Section 1 for Alternative 4 for a flow of 45,000 cfs

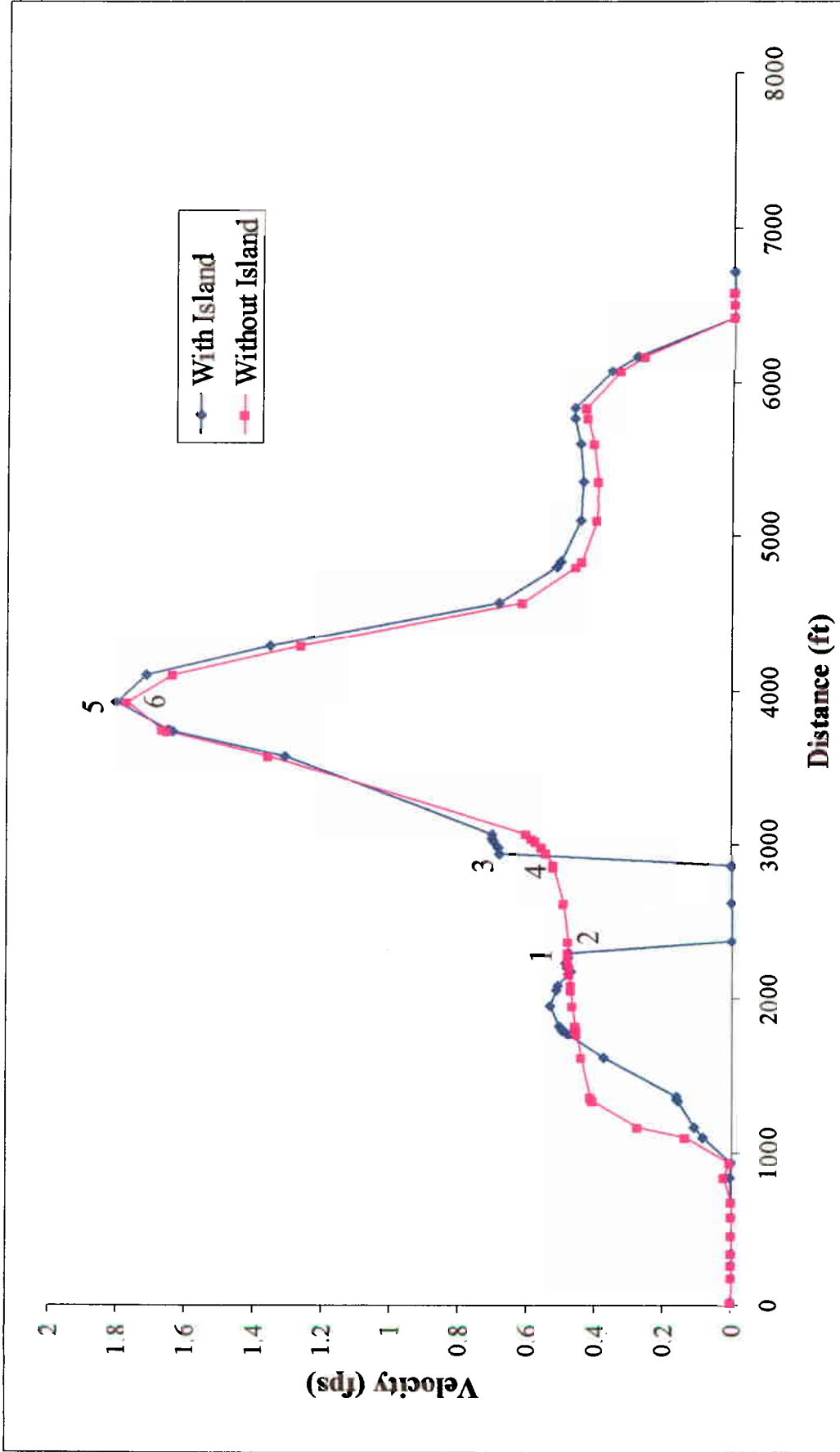


Figure 38. Lateral Velocity Distribution at Cross-Section 2 for Alternative 4 for a flow of 45,000 cfs

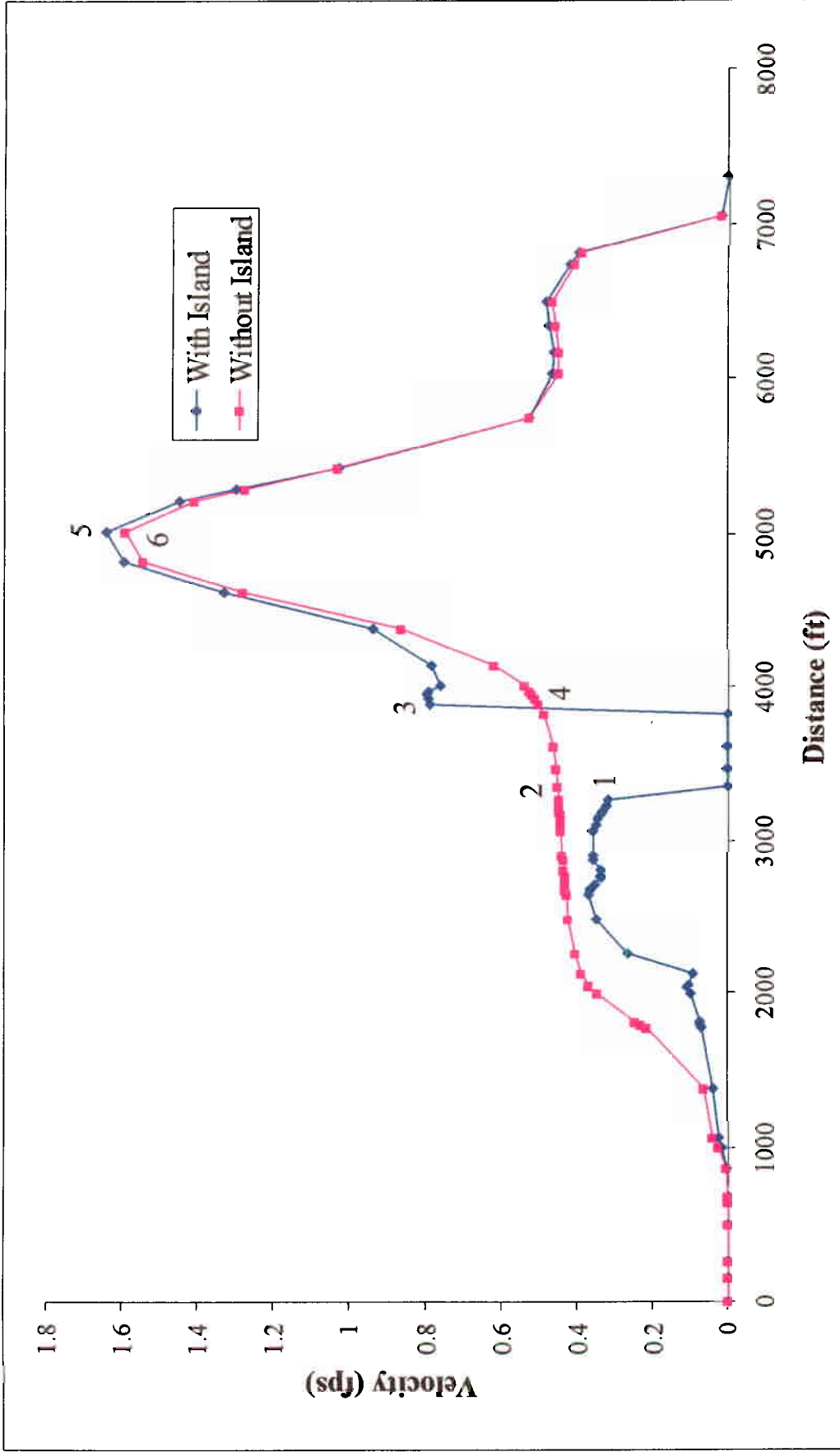


Figure 39. Lateral Velocity Distribution at Cross-Section 3 for Alternative 4 for a flow of 45,000 cfs

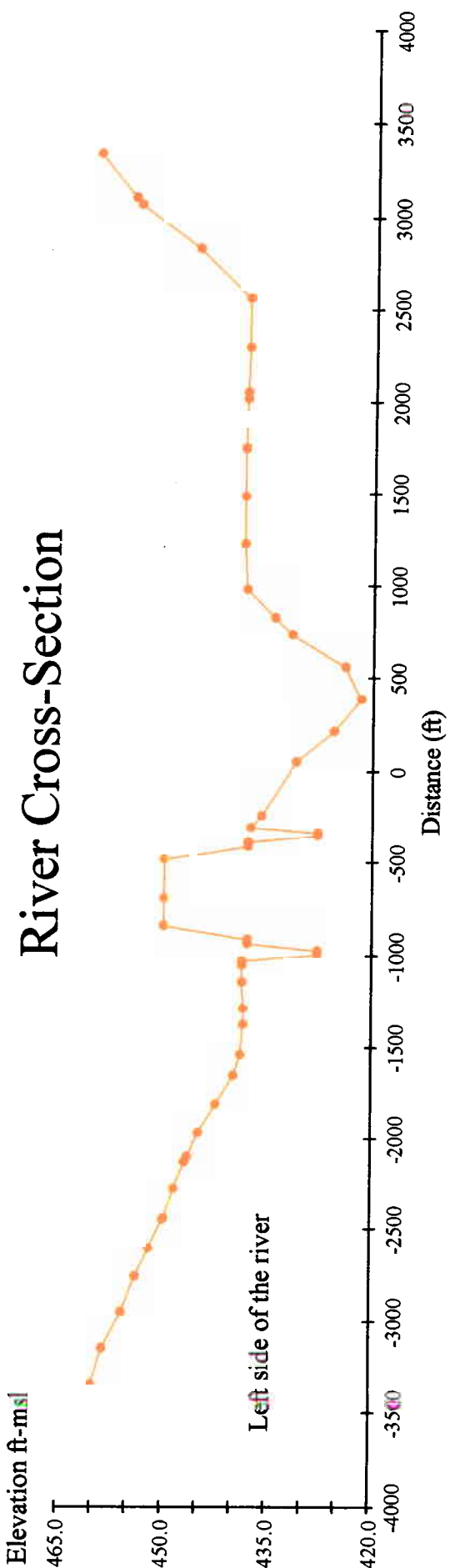
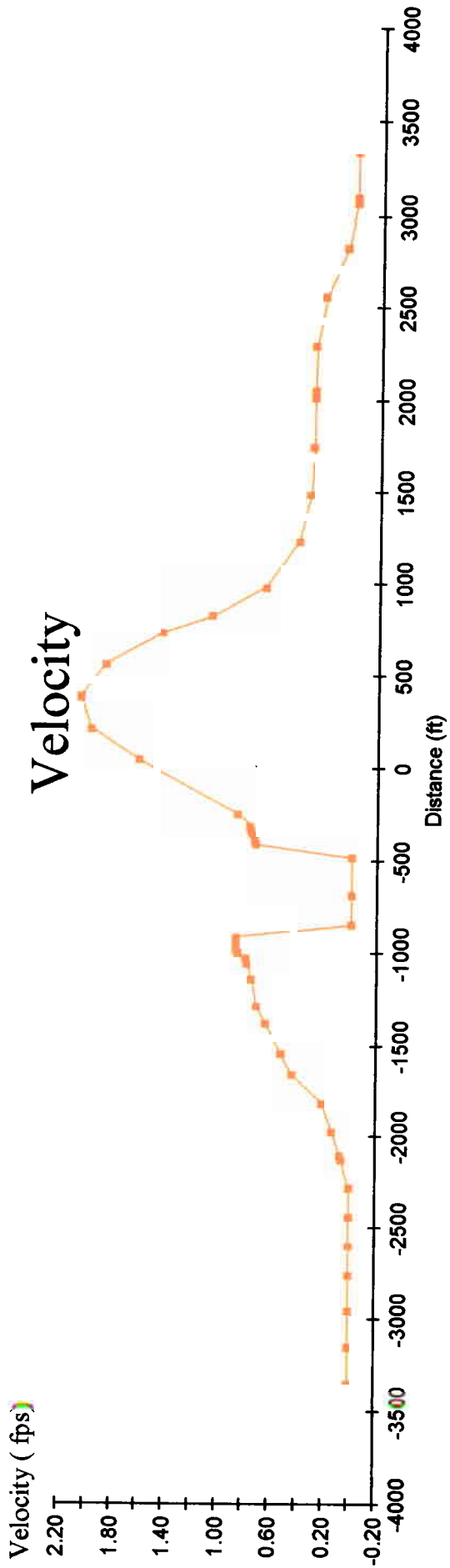


Figure 40. Lateral Velocity Distribution and River Cross-Sections at Cross-Section 1 for Alternative 4 for a flow of 45,000 cfs

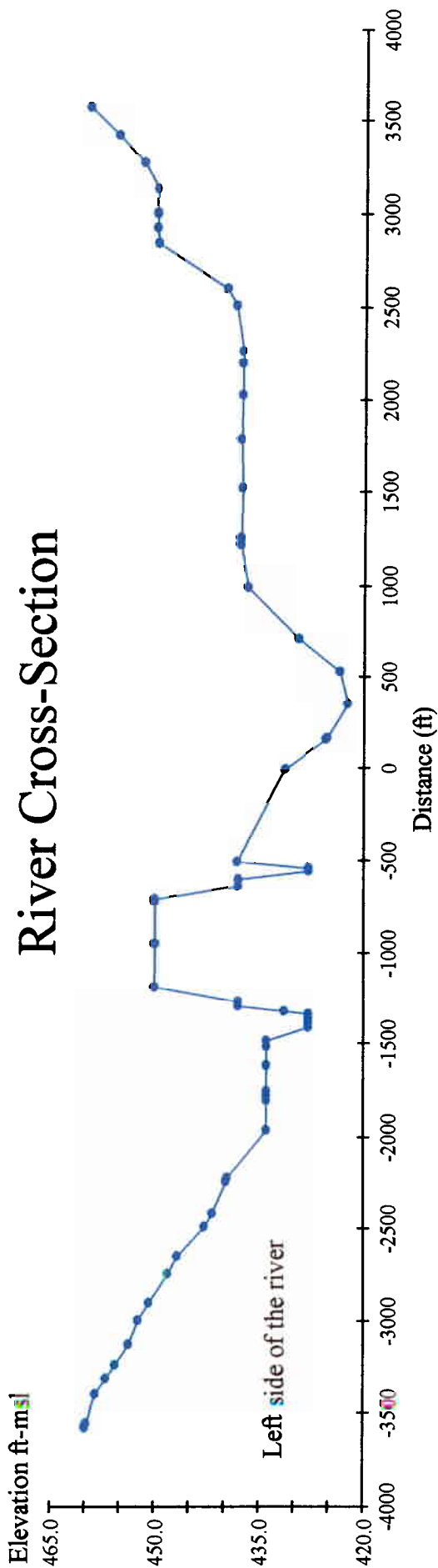
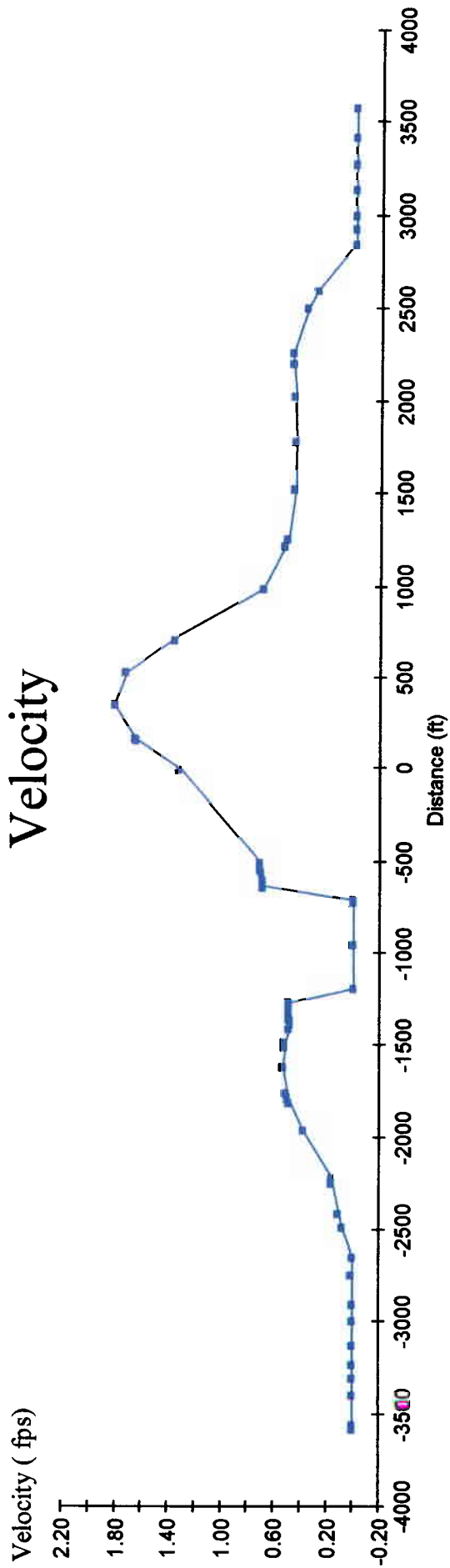


Figure 41. Lateral Velocity Distribution and River Cross-Sections at Cross-Section 2 for Alternative 4 for a flow of 45,000 cfs

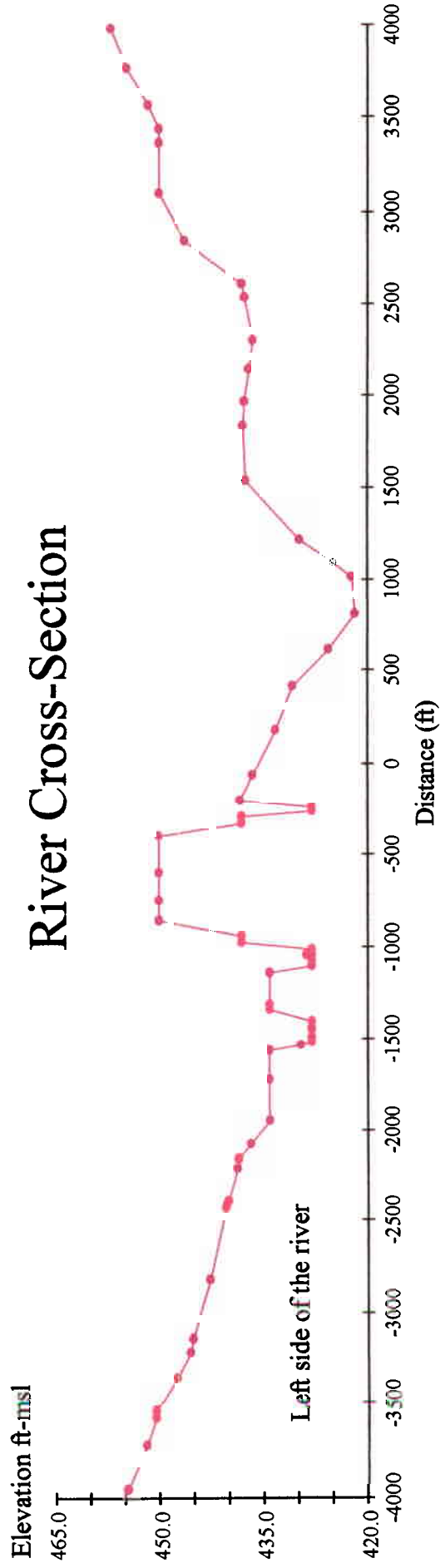
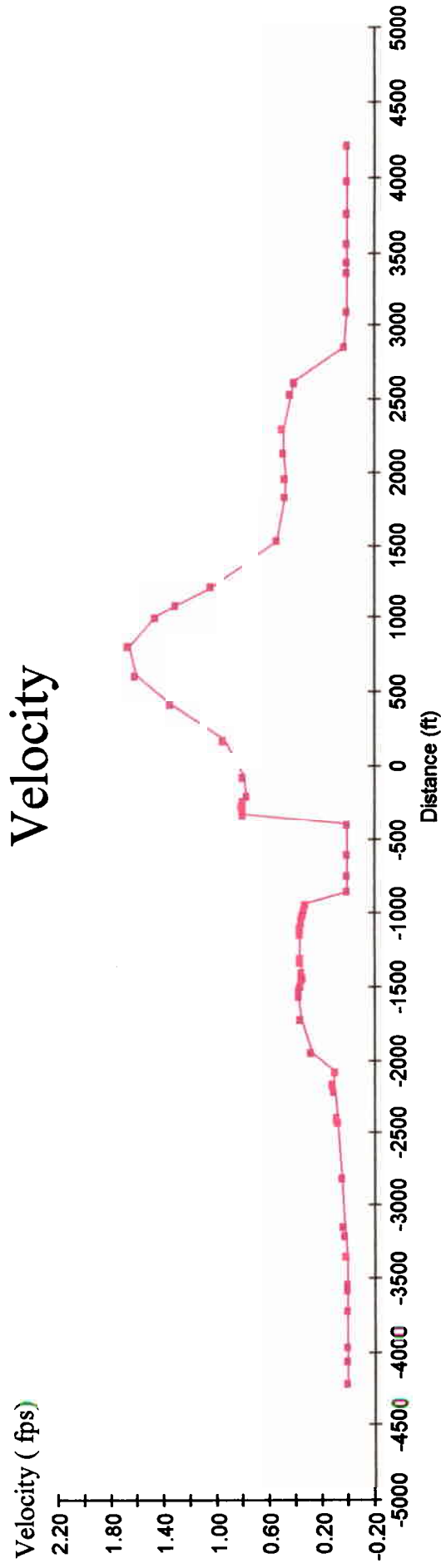


Figure 42. Lateral Velocity Distribution and River Cross-Sections at Cross-Section 3 for Alternative 4 for a flow of 45,000 cfs

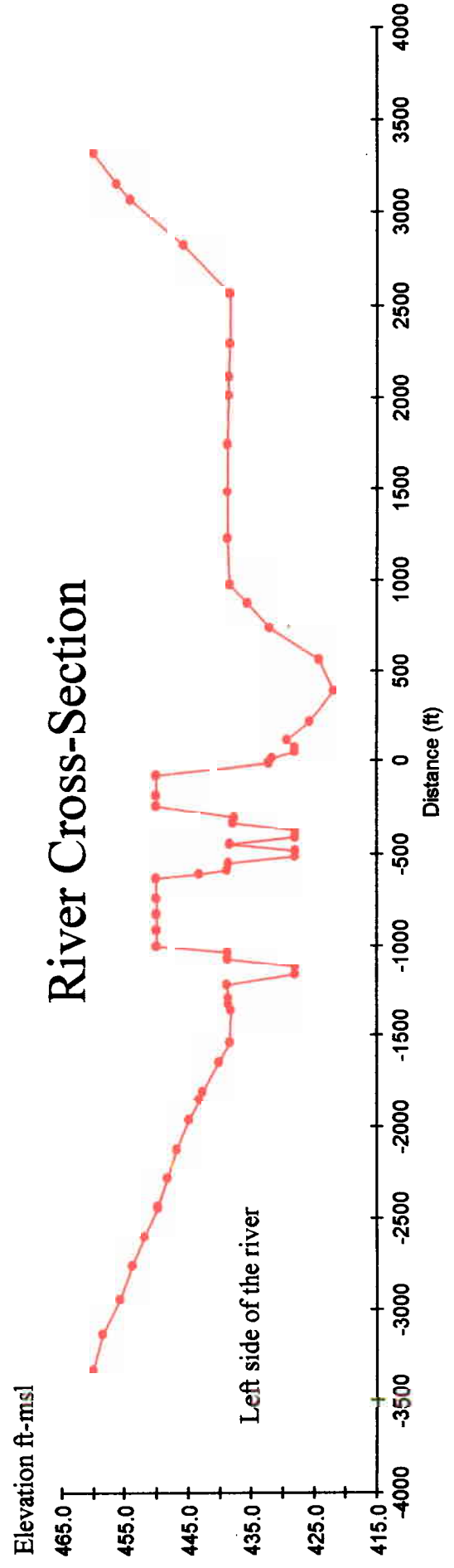
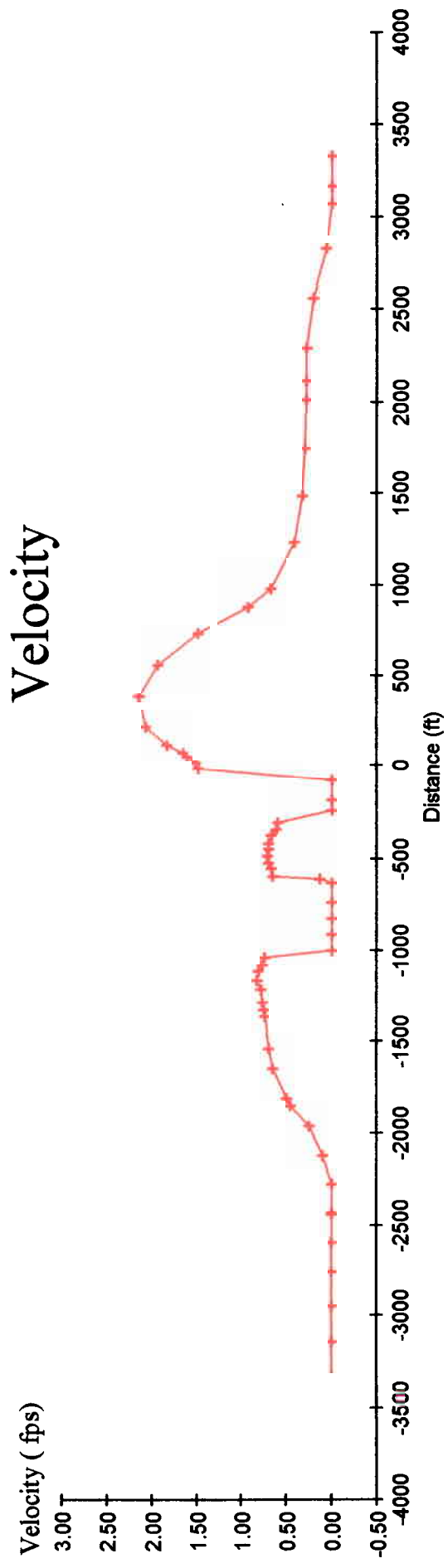


Figure 32. Lateral Velocity Distribution and River Section at Cross-Section 1 for Alternative 3 for a flow of 45,000 cfs